Spectral gamma ray characterisation of the Dongara Sandstone, Perth Basin, W.A; Applications to high-resolution correlation

Mark P. Di Bacco, BSc. (University of Adelaide)

This thesis is submitted in partial fulfilment of the requirements for the Honours Degree of Bachelor of Science (Petroleum Geology and Geophysics)

Australian School of Petroleum, University of Adelaide

November 2004

ABSTRACT

The northern Perth Basin has been a proven hydrocarbon province since the 1960s, however, little is known about the internal stratigraphy of the primary reservoir target – the late Permian Dongara Sandstone. Spectral gamma ray data has previously been used in the high-resolution correlation of sediments, but its potential in the Perth Basin has not been previously determined. The effectiveness of this technique is investigated here.

Spectral gamma ray (SGR) data were acquired from cores of the Dongara Sandstone using a hand-held gamma ray spectrometer. These data were combined with the relatively sparse wireline log SGR data available for the Dongara Sandstone. A study of the ratios of K, Th and U concentrations was first undertaken to determine whether SGR analysis was applicable in high-resolution correlation in the Dongara Sandstone. Core data was proven to be adequately precise for the comparison with wireline SGR data. It was confirmed that rocktypes could be clearly differentiated from one another on the basis of their SGR signatures. It was also proven that intra-formational character of the Dongara Sandstone could be identified from the SGR signatures, and that this character may have application in high-resolution correlation. Once the effectiveness of the SGR data for correlation had been demonstrated, the data were analysed with a suite of petrophysical software, creating a series of SGR composite logs for each well.

There was a good similarity between the SGR composite logs from rocks that had both wireline and core SGR measurements taken. This indicates that the core SGR can be confidently integrated with the wireline SGR data for use in interpretation. These SGR composite logs were used in high-resolution correlation of the Dongara Sandstone. Composite logs effectively display specific SGR signatures as a distinct colour, thus indicating the bulk mineralogy of the sediment and giving indications of distinct depositional facies. In particular, high-thorium intervals were interpreted as representative of beach facies due to the likely presence of the heavy mineral monazite. These facies were recognised in the composite logs, and in many cases,

facies could be correlated between wells in neighbouring fields. The stratigraphic and lateral extents of these facies were defined, enabling the construction of palaeogeographic maps for three chronologically separate Late Permian sediment packages. From these maps, the paleogeographic evolution was inferred. These maps indicate that the Dongara Sandstone is interpreted as having deposited on a series of back-stepping shorelines, depositing during a sea level transgression.

The sequential changes in facies distributions identified from SGR data can assist in defining the sequence stratigraphy of the Dongara Sandstone. With the internal architecture of the Dongara Sandstone defined, accurate predictions of reservoir distribution and quality can be made. This has important implications in the future exploration and exploitation of hydrocarbon accumulations within the Dongara Sandstone.

STATEMENT OF CONFIDENTIALITY

Due to a confidentiality agreement between Voyager Energy Ltd. and the Australian School of Petroleum, this thesis is not available for public inspection or borrowing until **November 2006.**

ACKNOWLEDGEMENTS

I would first like to thank my sponsor company Voyager Energy Ltd. for funding this study, and for assigning such friendly and helpful members of staff to assist me throughout my project. I must thank Dr Hamish Young for his mentoring throughout this project, and for being very patient and understanding. Hamish is also thanked for his assistance in core data acquisition. I would especially like to thank my supervisor, Catherine Gibson-Poole, for her numerous prompt and insightful comments throughout the progression of this study. I also thank supervisors Dr Tobias Payenberg and Andy Mitchell for their contributions. I would like to thank to Kerrie Deller, for her suggestions on this study. I also would like to thank the other honours and PhD students who gave moral support and encouragement throughout the year. Finally, I thank Mr Robert Charlebois from Crocker Data Processing, for his generosity and his assistance with the petrophysical software.

1 INTRODUCTION

1.1 Rationale

Recent oil discoveries, particularly at Hovea, Cliff Head and Jingemia, have proven the significant oil potential of the northern Perth Basin. The primary reservoir target within the Perth Basin is the Permian Dongara Sandstone. Despite production from this sand extending back to the 1960s, little is still known about its internal stratigraphy mainly due to:

- the poor quality of onshore seismic reflection data as a result of near surface carbonates,
- a serious lack of palynological data due to the dominance of clean sands, and;
- the unresolvability of conventional wireline logs.

As a result of these limitations, the correlation of the Dongara Sandstone has primarily been lithostratigraphic (H. Young, pers. comm., 2004). The spectral gamma ray (SGR) tool has proven itself as a high-resolution tool in sedimentary basins worldwide, with applications in correlation (Clare and Crowley, 2001) and sequence stratigraphy (Davies and Elliott, 1995); however, its potential has not been previously tested in the Dongara Sandstone.

The Dongara Sandstone commonly contains high gamma ray ('hot') intervals, thought to be due to the concentration of the heavy mineral monazite (Rasmussen et al., 1989; WAPET, 1996). The thorium content of monazite means the presence of this mineral is easily detectable as thorium-rich intervals in SGR wireline logs (Adams and Weaver, 1958). The distribution of these hot sands may be related to facies, however, if this concept has been investigated in the Perth Basin, the results have not been published to date. Wireline SGR data is sparse across the Perth Basin, but many wells contain cores cut through the reservoir interval. A handheld gamma ray spectrometer can provide SGR data from cores, thus increasing the size of the SGR

dataset, and extending the potential for high-resolution correlation within the Dongara Sandstone.

With the development of a high-resolution correlation framework for the Dongara Sandstone, the internal sequence stratigraphy can be resolved. This should lead to a better understanding of the internal architecture of the reservoir, which will in turn assist in developing more efficient exploitation strategies and improve the focus of future exploration programs.

1.2 Research Aims

This thesis aims to determine the suitability of both core-obtained and wireline log SGR data as a high-resolution facies determination and correlation tool within the Dongara Sandstone. The effectiveness of core SGR data as a substitute for wireline SGR data will be assessed. Further analysis of these data will validate whether Perth Basin rocktypes can be differentiated on the basis of their SGR signature.

If this technique proves effective, it will aid in building up a sequence stratigraphic framework for the Dongara Sandstone, which is important for developing a better understanding of the reservoir for future exploration and field development. If this is the case, Voyager Energy will consider running SGR logs in all future exploration wells.

1.3 Regional Setting and Location of Study Area

The Perth Basin is a 1000km long north-south trending trough, which lies on the southwest coast of Western Australia (Fig. 1.1). The basin contains sediments ranging in age from Ordovician to Recent (Song and Cawood, 2000; Thomas and Barber, 2004). It comprises of a series of northerly-striking sub-basins, covering an area of approximately 45,000km^2 onshore and 55,000km^2 offshore (Harris et al., 1994; Song and Cawood, 2000). The northern Perth Basin, about 230km north of Perth, is the focus for this study. Exploration well Wicherina 1 and the Woodada gas field represent the northern and southern limits respectively, covering an area of approximately

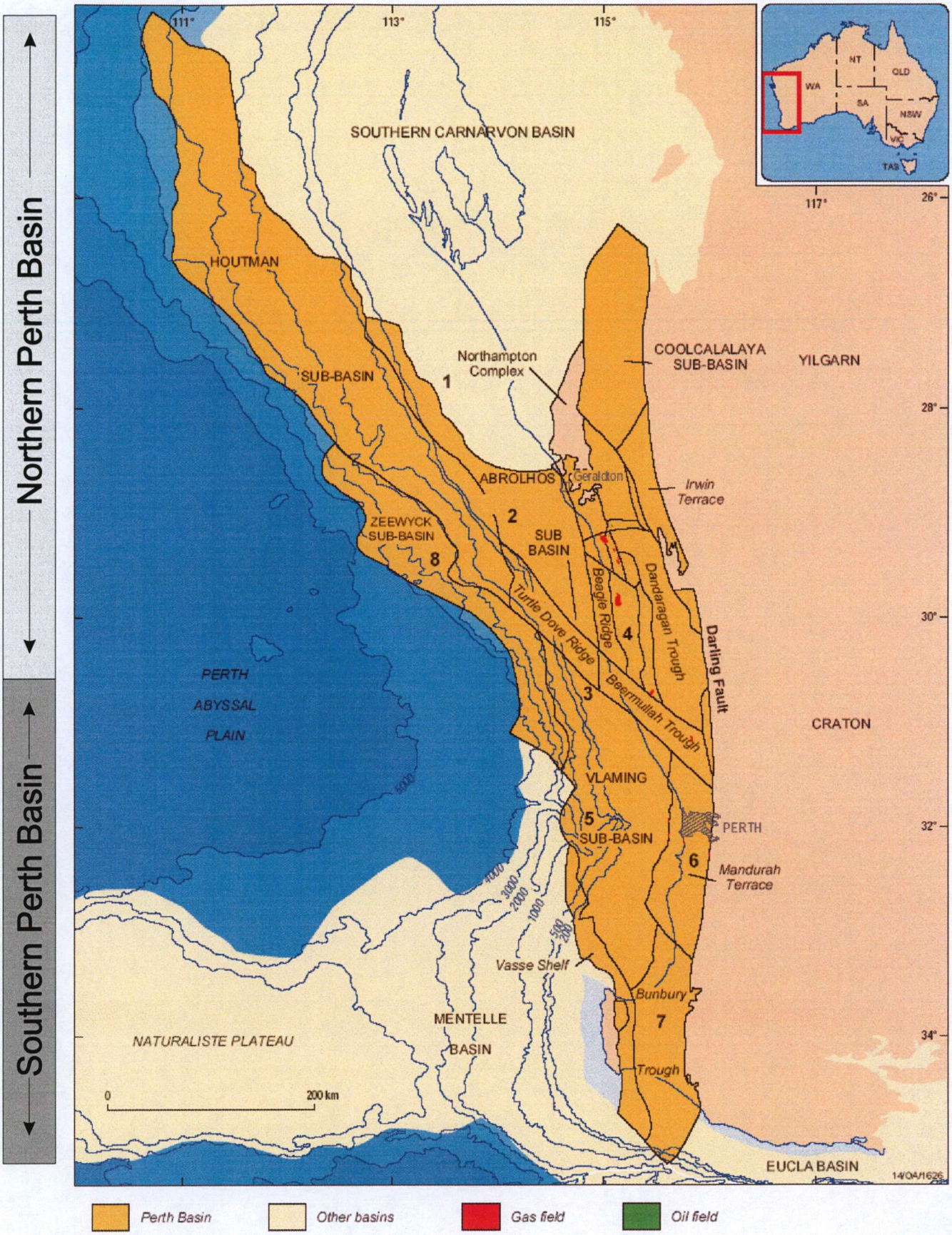

Figure 1.1 Location Map of the Berth Basin (adapted from Geoscience Australia, 2004)

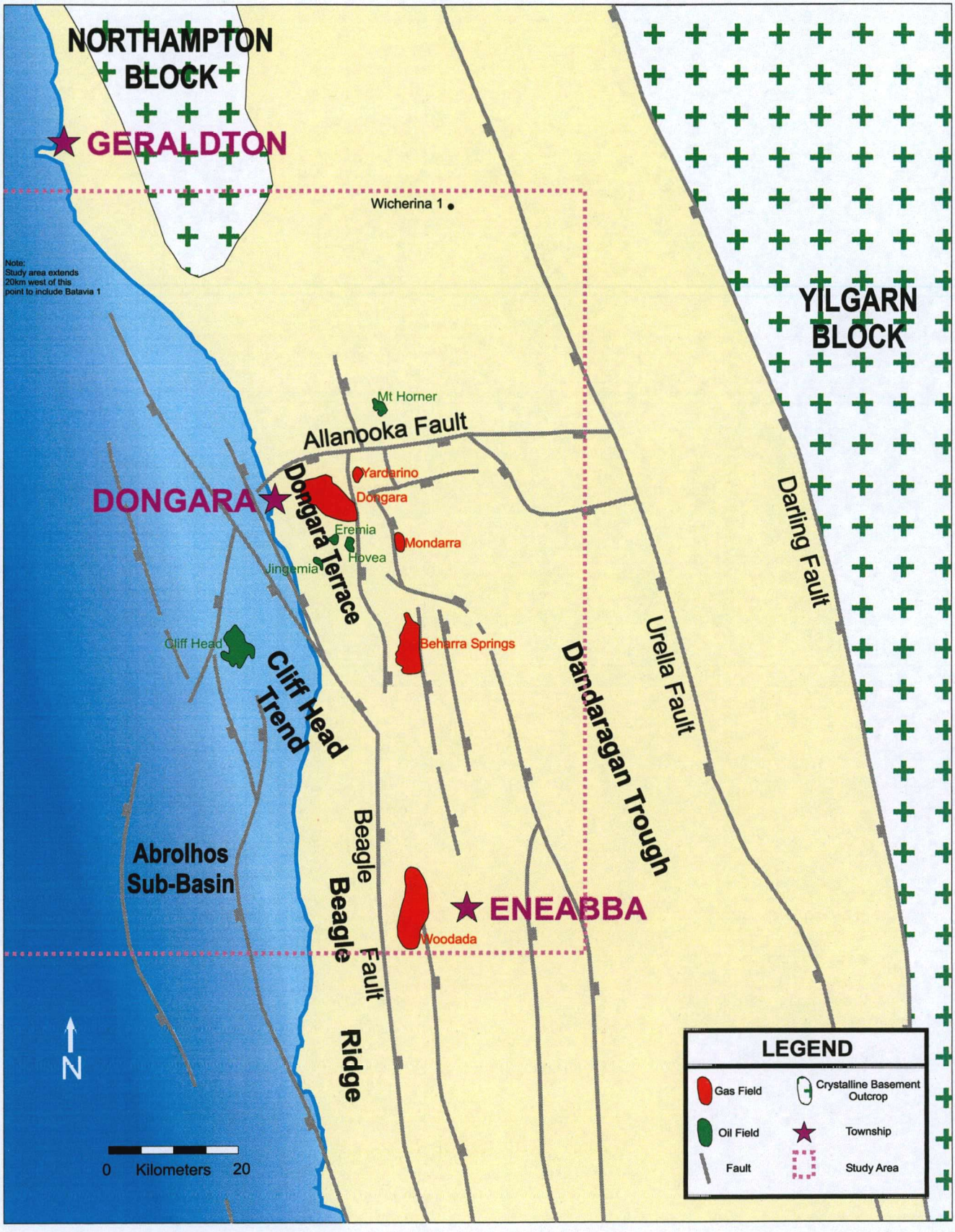

Figure 1.2 Structural map of the northern Perth Basin (Adapted from Buswell et al., 2004; Thomas and Barber, 2004)

10,800km^2 (Fig. 1.2). Within this area, the Dongara Sandstone is thought to represent the transition from a fluvial facies in the north through to a carbonate facies in the south (Mory and Iasky, 1996).

1.4 Exploration History

The exploration of the Perth Basin commenced in 1951 when the Bureau of Mineral Resources (BMR) conducted gravity surveys over the onshore northern Perth Basin. West Australian Petroleum Pty Ltd (WAPET) and the BMR drilled numerous stratigraphic wells in the basin, and in 1961, WAPET drilled the first wildcat well, Eneabba 1 (Owad-Jones and Ellis, 2000). In 1963, WAPET discovered a significant accumulation of natural gas in the Yardarino gas field (WAPET, 1996). This discovery boosted interest in the basin, and resulted in the discovery of the Dongara and Mt Horner fields in 1965 and the Mondarra field in 1968 (Mory and Iasky, 1996). Following these discoveries, there was little exploration activity in the basin until 1980, when smaller companies became increasingly active.

For many years the Perth Basin had been regarded as gas prone; however, the discoveries of the Hovea, Jingemia, Eremia and Cliff Head oil fields in the last decade have dispelled this myth. Subsequent exploration in the Perth Basin has been vigorous, with many small to medium-sized companies presently holding much of the onshore and offshore exploration acreage (H. Young, pers. comm., 2004).

1.5 Available Dataset

Most of the exploration wells in the northern Perth Basin are located onshore, with many of these centred on the Dongara Terrace (Fig. 1.2). Offshore wells are mostly recent additions, and are generally centred southwest of the Dongara Terrace, near the Cliff Head oil field (Fig. 1.3). Little exploration has occurred in the southern Perth Basin. It is considered to be a frontier province, and has not been incorporated into this study. A total of 29 wells from the northern Perth Basin have been investigated during this particular study. The location of these wells is shown in Figure 1.3. Of these, 23 have core (Table 1.1)

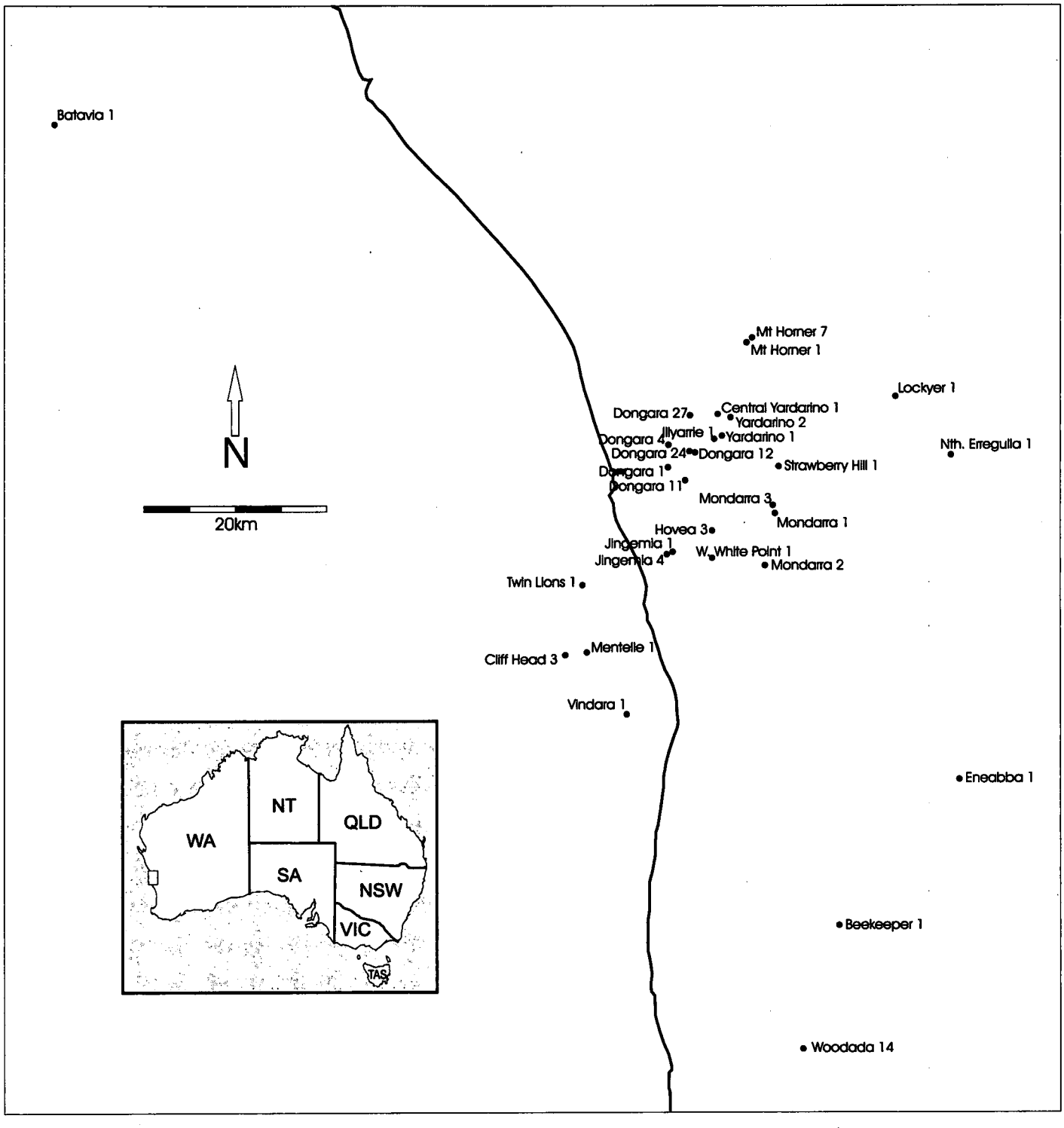

Figure 1.3 Location map of the wells used in this study

Table 1.1. List of wells and data used in this study

Well Name	Wireline SGR data	Cores Available	Comments
Batavia 1	×	✓	
Beekeeper 1	×	✓	
Central Yardarino 1	✓	✓	
Cliff Head 3	✓	✓	
Dongara 1	×	✓	
Dongara 4	×	✓	
Dongara 11	×	✓	
Dongara 12	×	✓	
Dongara 24	×	✓	
Dongara 27	×	×	Wireline GR Only
Hovea 3	×	✓	
Illyarrie 1	×	×	Wireline GR Only
Jingemia 1	✓	×	
Jingemia 4	×	✓	
Lockyer 1	×	✓	
Mentelle 1	✓	×	
Mondarra 1	×	✓	
Mondarra 2	×	✓	
Mondarra 3	×	✓	
Mt Horner 1	×	✓	
Mt Horner 7	✓	✓	
Nth Erregulla 1	×	✓	
Strawberry Hill 1	×	✓	
Twin Lions 1	✓	×	
Vindara 1	✓	×	
W White Point 1	×	✓	
Woodada 14	×	✓	
Yardarino 1	×	✓	
Yardarino 2	×	✓	

✓ -Dataset available × -Dataset not available

1.6 Background Theory

1.6.1 Gamma Rays

Gamma ray (GR) wireline logs have been used for many years in the petroleum industry, and are arguably the principal tool for lithology determination and correlation. The GR tool measures natural gamma ray emissions from the rocks immediately surrounding the wellbore. These emissions are mostly derived from the chemical elements potassium (K), thorium (Th) and uranium (U) (Adams and Weaver, 1958). These elements are commonly found in sedimentary rock-forming minerals, and have isotopes that are radioactively unstable (^{40}K, ^{232}Th and ^{238}U respectively) (Adams and Weaver, 1958). The decay of these unstable isotopes causes the creation of

a new daughter element, at the same time releasing a photon of gamma radiation whose energy is specific to that of the parent element (Fig. 1.4). Potassium (^{40}K) decays directly into its stable daughter element argon, with the emission of a gamma ray having an energy of 1.67 MeV (Fig. 1.4). Thorium and uranium decay via complex pathways until they become a stable lead isotope. These radioisotopes are measured indirectly by detecting the distinct emissions of their daughter isotopes, Thallium (^{208}Tl) and Bismuth (^{214}Bi) respectively (Baker Atlas, 1992).

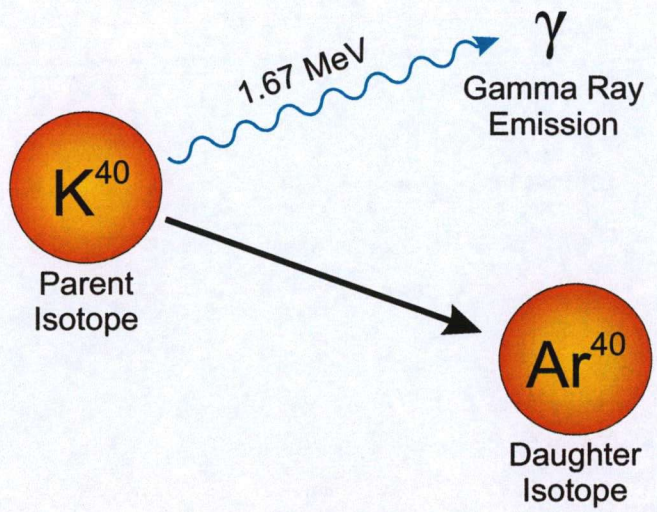

Figure 1.4 Schematic diagram illustrating the decay of the potassium^{40} isotope into its daughter isotope argon^{40}.

Potassium is common in many types of sediment that contain feldspar, mica, clays or chloride salts (Ruffell and Worden, 2000). Thorium and uranium are commonly found loosely bound to organic matter, or sorbed to the mineral surfaces of clays and iron oxides (Wilford et al., 2001); however, they may also be present in the crystal lattice of minerals, particularly resistant heavy minerals like monazite and zircon (Adams and Weaver, 1958; Rasmussen et al., 1989).

The total gamma ray (GR) wireline log measures the combined gamma radiation from all three elements (K, Th and U), whereas spectral gamma ray (SGR) wireline logs indicate the amount of each individual element contributing to the total radioactivity (Rider, 1996). The intensity of this

gamma radiation can be accurately counted using a spectrometer, and from this the concentration of the parent isotope (K, Th or U) can be inferred. Due to its relative crustal abundance, K is generally measured in per cent (%), whereas Th and U are commonly present in much smaller concentrations and as such are measured in parts per million (ppm). The relative concentrations of the three elements (K, Th and U) can give indications of clast and matrix mineralogy, which can be extremely useful when correlating sand bodies (Rider, 1996; Clare and Crowley, 2001; Baker Atlas, 1992).

Spectral gamma ray analysis has been used in many geological applications, ranging from rapid soil mapping to correlation and reservoir characterisation and palaeoclimate studies (Ruffell and Worden, 2000; Wilford et al. 2001; Clare and Crowley, 2001; Svendsen and Hartley, 2001). Saunders et al. (1993) even used the SGR signature of surface soils to remotely identify petroleum accumulations at depth. Of particular relevance to this study was the use of SGR data by Davies and Elliott (1995), who used outcrop SGR readings as a high-resolution correlation tool in a sequence stratigrapic analysis of fluvio-deltaic sediments. This study used ratios of K, Th and U to determine key sequence stratigraphic surfaces, such as maximum flooding surfaces and erosional unconformities.

1.6.2 Heavy Minerals

Heavy minerals (such as monazite) are preferentially concentrated in beach sediments because of entrainment equivalence (Reid and Frostick, 1985). This property means that it is relatively difficult to entrain heavy mineral grains back into the transporting medium once they are deposited from the water column (Reid and Frostick, 1985; Morton and Hallsworth, 1999). Therefore, quartz (which is comparatively lighter) would be entrained preferentially back into the transporting medium, leaving behind the heavy mineral grains. This mechanism is further exaggerated by the fact that heavy minerals are smaller in size than the surrounding quartz grains (due to their hydraulic equivalence with larger quartz grains). The heavy mineral grains therefore lie in the interstices between the quartz grains, thus further reducing their ability to be

entrained back into the transporting medium (Reid and Frostick, 1985). This mechanism is seen to operate in beach environments where the constant agitation of the shoreface sediments by the breaking waves concentrates any heavy minerals present. The entrainment equivalence property of heavy minerals is considered the principal factor for generating placer deposits (Reid and Frostick, 1985; Morton and Hallsworth, 1999).

The gamma ray count is high in monazite-rich sands, superficially complicating GR wireline logs (WAPET, 1996). Radioactive sands are known in the petroleum industry as "hot sands". A diagnostic feature of monazite is that it emits gamma rays characteristic of thorium. Therefore, sands with a high thorium anomaly can be quite confidently attributed to the presence of monazite. One such example of a monazite-rich hot sand is seen in the wireline SGR logs of Jingemia 1 (Fig. 1.5).

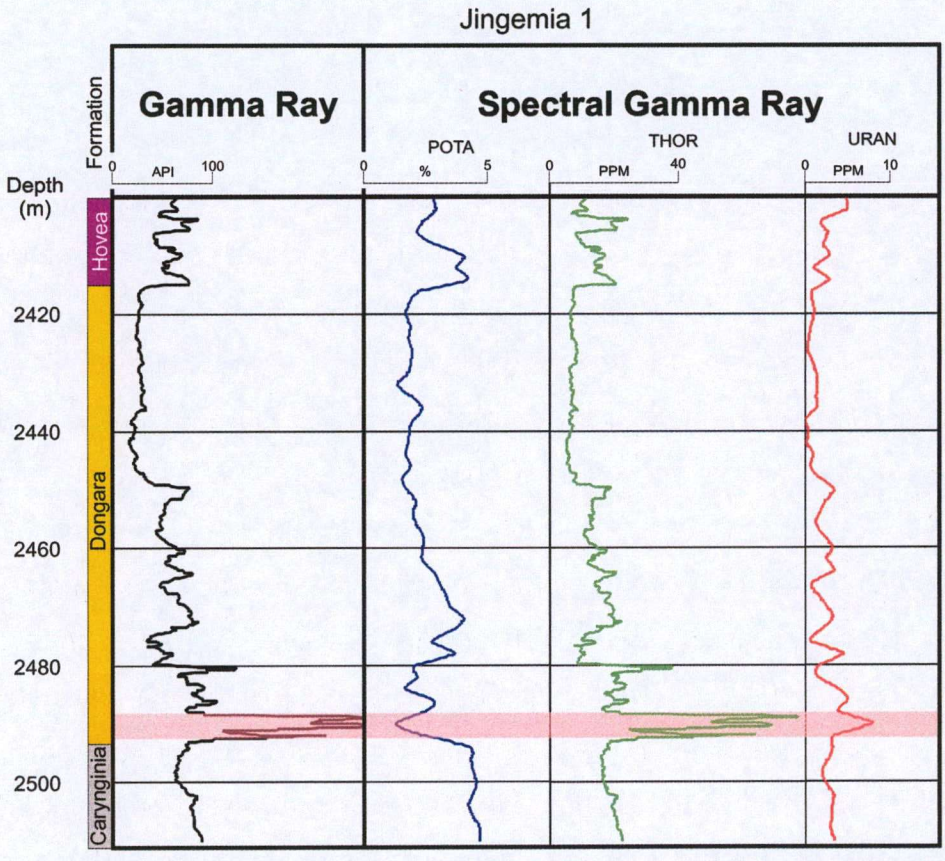

Figure 1.5 Jingemia 1 SGR wireline logs. Note that the hot gamma ray zone (highlighted in pink) is the result of a thorium anomaly. Thus, it can be deduced that the reason for the high radioactivity of this interval is due to appreciable amounts of the heavy mineral monazite.

2 GEOLOGICAL SETTING

2.1 Tectonic History

The Perth Basin formed as a result of the rifting that occurred during the separation of Australia and Greater India during the break up of the Gondwanan supercontinent (Song and Cawood, 2000). The sedimentary succession of the Perth Basin demonstrates that rifting occurred in two main phases, with initial rifting occurring in the Permian and subsequent rifting occurring in the latest Jurassic-earliest Cretaceous (Song and Cawood, 2000; Mory and Iasky, 1996). The north-south structural grain of the Perth Basin is believed to be inherited from the underlying Precambrian crystalline basement of the Yilgarn Craton (Harris et al, 1994).

The initial Permian rift event saw much of the early extension taken up by a series of northerly striking planar and listric faults. This earliest phase of rifting is demonstrated by thickening of Permian sediments in the hanging wall of the northerly trending Mountain Bridge fault (Song and Cawood, 2000). The second phase of rifting represents the final stages of break up between the Australian and Indian blocks. The master faults (which accommodated the extension in the Permian) were reactivated in this second rifting phase. Again, sedimentary thickening in the hanging walls of these faults indicate the renewed rifting (Song and Cawood, 2000).

The eastern boundary of the Perth Basin is currently defined by the Darling-Urella fault system. Song and Cawood (2000) state that 6km of displacement has occurred on this fault since its inception in the Permian.

2.2 Stratigraphy of the Northern Perth Basin

The Perth Basin is still regarded as a relatively frontier basin, with geological interpretations constantly evolving as more data is acquired. The most recent papers are of most use, with Mory and Iasky (1996) outlining in detail the stratigraphy of the northern Perth Basin. Stratigraphic interpretations are of

restricted value, especially in old publications and vintage well completion reports. The stratigraphic summary presented here stems from Mory and Iasky (1996) except where noted. However, only the formations of interest to this study, which range from Permian to Triassic in age, are described. The stratigraphic column is shown in Figure 2.1.

2.2.1 Early Permian

The High Cliff Sandstone is a conglomeratic sandstone with minor siltstone. It is interpreted to have been deposited in a shallowing marine environment. Outcrop of this formation contains hummocky cross-stratification and wave ripple sedimentary structures. This sandstone grades upwards into a silty coal-bearing unit named the Irwin River Coal Measures. Outcrop of this formation commonly displays shale rip-up clasts and coalified plant remains, and is interpreted to mark the transition from a shoreface depositional environment into a terrestrial fluvial environment. The coal from this formation may have sourced the gas accumulations throughout the Perth Basin. The Irwin River Coal Measures extend transitionally into the overlying Carynginia Formation. This is a dark carbonaceous and micaceous siltstone with minor coarse-grained clastic lenses and occasional glacially transported erratic boulders up to 1.5m wide. This formation is interpreted to represent a relative sea level rise in the Early Permian. The interpreted depositional environment is thought to be shallow marine conditions in the final stages of a glacial retreat. The lower units of the Carynginia Formation contain erratic boulders, however, further up in the sequence, these boulders decrease in size and frequency, consistent with the palaeoenvironment being the final stages of glacial conditions.

The boundary between the Carynginia Formation and overlying sediments is identified as unconformable on the basis of several missing palynomorph zones. This surface is known as the mid Permian unconformity, and can be correlated across the whole of the northern Perth Basin.

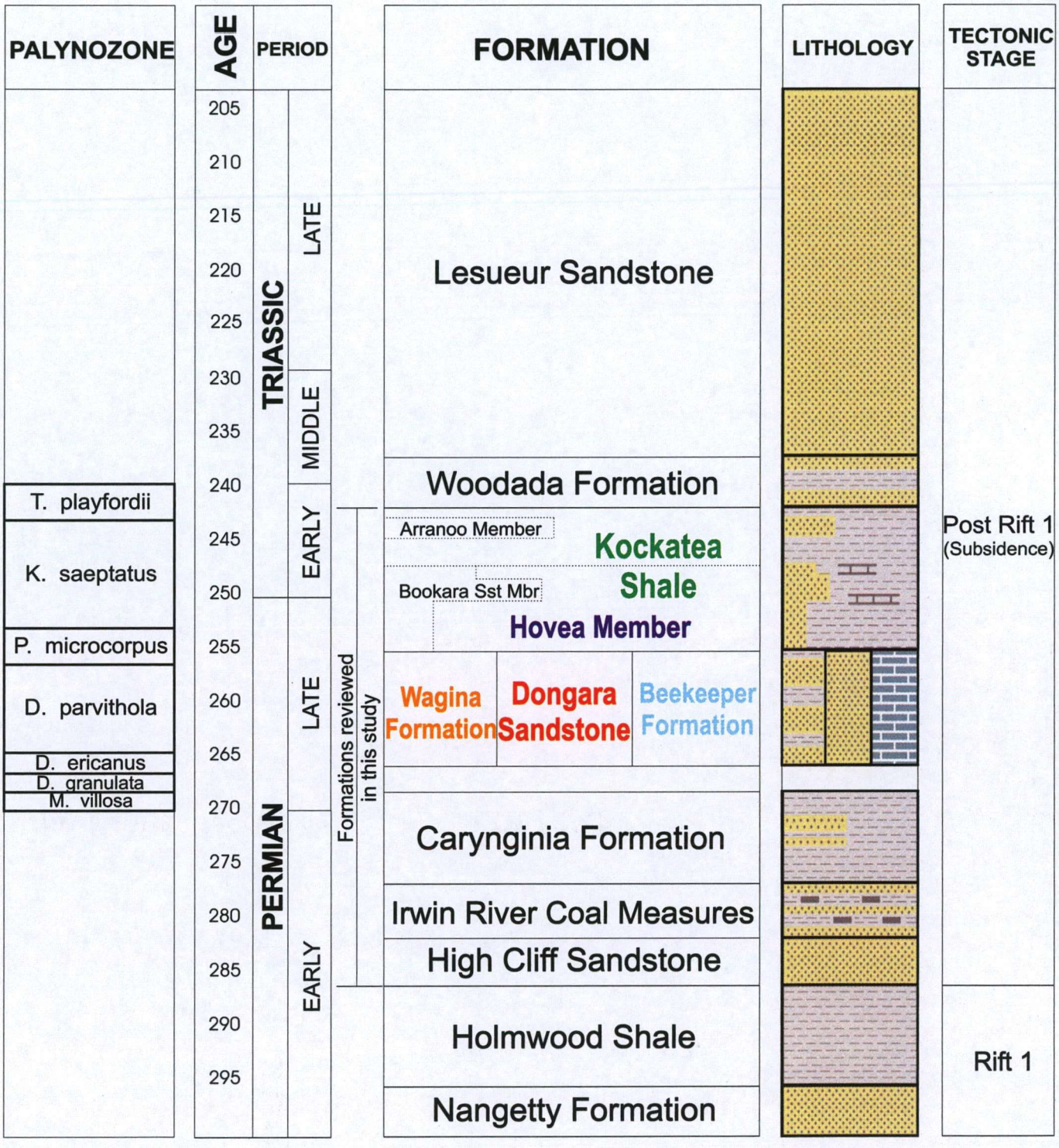

Figure 2.1 Stratigraphic column of the northern Perth Basin (adapted from Song and Cawood, 2000; Thomas and Barber, 2004)

2.2.2 Late Permian

Late Permian sediments of the Wagina Formation, Dongara Sandstone and the Beekeeper Formation were deposited following the mid Permian hiatus. These formations are coeval, and represent fluvio-deltaic, shoreface and marine environments respectively.

The Wagina Formation is a fine to medium-grained, clayey to pebbly sandstone with minor conglomerate lenses and carbonaceous silts. From structures seen in outcrop and core, the depositional environment of the Wagina Formation is thought to be a proximal delta.

The Wagina Formation undergoes a lateral facies change to the south, grading into the Dongara Sandstone. The Dongara Sandstone is interpreted as a shoreface sandstone, and is described in detail later in this chapter.

The southwest extent of the Dongara Sandstone contains interfingering limestone beds. This lithology change represents the transition from the Dongara Sandstone into the Beekeeper Formation. This observation supports the premise that the depositional environment extends into the marine realm, and that these units are at least partly coeval.

The Beekeeper Formation is a mixed clastic and carbonate unit representing the most distal part of its coeval Dongara Sandstone. This formation is generally composed of rudstones/grainstones and wackestones/packstones with minor mudstones (Just, 2002). The high proportion of fossiliferous carbonate material with calcareous sandstone and shales, all containing acritarchs, suggest an open marine depositional environment. Post-depositional diagenesis has occluded all primary porosity in the limestone, however, dolomitization and fracturing have generated secondary porosity, making it a viable gas reservoir in the Woodada gas field (Just, 2002).

2.2.2.1 The Dongara Sandstone

The Dongara Sandstone is a quartz-rich, silty to pebbly sandstone, which has had many names in the past (including the Basal Triassic Sandstone, despite

being Late Permian in age). This sandstone is the major hydrocarbon reservoir target in the northern Perth Basin, due to its lateral continuity, excellent reservoir characteristics and its presence below a regional seal. The distribution of the Dongara Sandstone exhibits a general thinning to the west, from >330m adjacent to the Darling-Urella fault system in the east to 60m at the Dongara Field in the west.

The interpreted depositional environment of the Dongara Sandstone is not very well constrained, however, it is believed to range between proximal deltaic to shallow marine. The reservoir characteristics of the Dongara Sandstone are excellent, with porosities nearing 25% and typical permeability of 200mD (WAPET, 1996). The beach facies are the best reservoir quality (in terms of permeability) due to their coarse grain size and low authigenic clay content (Owad-Jones and Ellis, 2000)

Sediments of the Dongara Sandstone were first believed to have been derived from the weathering of the nearby Precambrian Yilgarn Craton and the North Hampton Complex basement blocks, mixed with the reworked material of younger Phanerozoic sediments (Rasmussen et al., 1989). Later work on zircon provenance by Cawood and Nemchin (2000) showed that these sediments were lacking significant amounts of Archaean detritus, thus excluding the Yilgarn Craton as a major potential sediment source. Cawood and Nemchin (2000) describe the Dongara Sandstone as having zircon ages that broadly range from Archean to Palaeoproterozoic, but most of the detritus is Mesoproterozoic (Fig. 2.2). Therefore, a mixed provenance is most likely for the Dongara Sandstone. De Broekert et al. (2004) postulate that the Proterozoic Albany-Fraser-Wilkes and Pinjarra Orogens shed sediments onto the southwest Yilgarn Craton during Early Permian glaciations, which were later reworked into the emerging Perth Basin during Late Permian – Early Cretaceous rifting. This theory is supported by the zircon ages of the late Permian Perth Basin sediments.

Sections within the Dongara Sandstone contain anomalous amounts of the radioactive heavy mineral monazite (Rasmussen et al., 1989). Monazite is a

rare earth phosphate with a specific gravity between 4.8 and 5.5 g/cm^3 and is a common accessory mineral in granites and gneisses (Prinz et al., 1978). Monazite is particularly resistant to chemical weathering and as such is a common component of the heavy mineral assemblage in sandstones (Morton and Hallsworth, 1999). In sufficient concentrations, this mineral accumulation complicates the GR wireline log signature (WAPET, 1996). However, a monazite signature may be diagnostic of certain depositional facies, since monazite is commonly found as a placer mineral in beach deposits (Morton and Hallsworth, 1999).

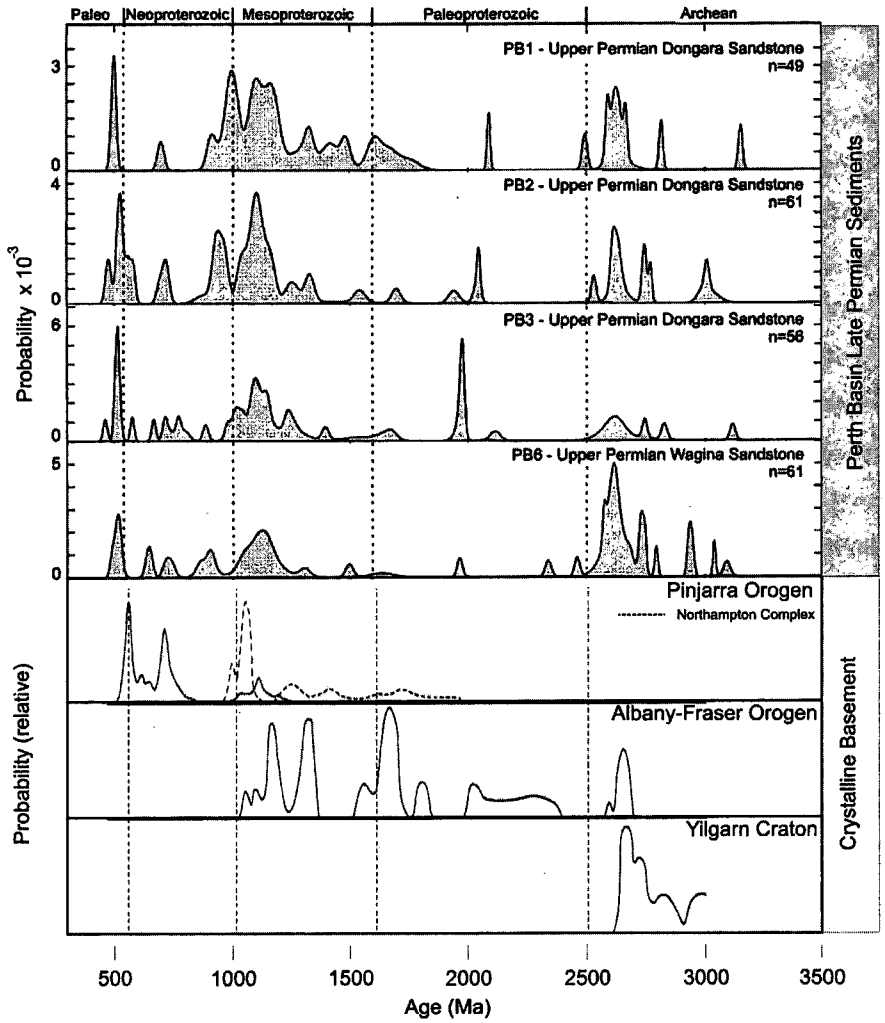

Figure 2.2 Zircon ages of the crystalline basement blocks of Western Australia, and the late Permian sediments of the northern Perth Basin (Adapted from Cawood and Nemchin, 2000; De Broekert et al., 2004)

2.2.3 Triassic

The earliest Triassic is marked by the deposition of the Kockatea Shale. This shale is considered to be the regional seal across the whole of the northern Perth Basin. The main oil charge for Perth Basin discoveries is interpreted to have come from a thin subsection of the Kockatea Shale known as the Hovea Member (Thomas and Barber, 2004). The Hovea Member sits stratigraphically above the Dongara Sandstone, which, as previously stated, is the primary reservoir in the northern Perth Basin.

The Kockatea Shale is believed to have been deposited during a marine transgressive and regressive cycle. The laminated, fossiliferous, organically-rich Hovea Member was deposited during the transgressive cycle and the remainder of the Kockatea Shale was deposited during the subsequent highstand systems tract (Thomas and Barber, 2004).

The Hovea Member can be further subdivided into inertinitic and sapropelic intervals, and are believed to represent the early and late stages of the transgressive cycle (Thomas and Barber, 2004). The inertinitic interval contains total organic carbon (TOC) values of up to 3%, however, the dominant organic maceral is inertinite, meaning the oil source potential is low. The interval represents a suboxic depositional environment in which only limited organic matter was preserved.

The sapropelic interval of the Hovea Member is organically-rich and extremely oil-prone with TOC values typically up to 5%. The sapropelic interval is normally 10-40 m thick across the onshore northern Perth Basin, and is regarded as one of the best oil source rocks ever identified in Australia (Thomas and Barber, 2004). This interval is characterised by finely laminated, alternating beds of dark shales and thin limestone bands (Thomas and Barber, 2004). The shales are fossiliferous in some parts, and commonly contain framboidal pyrite and pyrite replacement in fossil chambers (Thomas and Barber, 2004). The limestone bands frequently include small stromatolite colonies and algal mats. There is no evidence of bioturbation in either the

shales or the limestone beds, and this is congruent with the notion that they were deposited in an anoxic, sheltered sea (Thomas and Barber, 2004).

The Hovea member is topped by a thin limestone interval generally less than 5m thick. This interval represents the peak of marine transgression, and is an excellent marker bed due to its easily identifiable sonic and resistivity wireline log characteristics and due to its lateral extent across most of the northern Perth Basin (Thomas and Barber, 2004).

The Hovea member grades upwards into the more organically lean Kockatea Shale, which is thought to contribute very little as a source to the total trapped amount of hydrocarbons in the basin. The mid Kockatea Shale has a TOC generally below 0.5%, and as a result, its source potential is low (Thomas and Barber, 2004).

The Kockatea Shale is characterised in outcrop as a red to browny-buff coloured, ferruginous shaly siltstone with fine-grained sandstone intervals. The fine sand intervals represent storm periods, and in some instances, their thickness and lateral extent warrant them member status (i.e. Arranoo Member). The presence of these sands within the Kockatea Shale indicates that the continental shelf at the time of deposition lay within the storm weather wave base. Individual sand beds in the Kockatea Shale are generally less than 10cm thick, and display cross-bedding, asymmetric ripples and trail marks. The features of these sand bodies within the Kockatea Shale indicate that it was deposited on a shallowly dipping continental shelf, where sediments are actively influenced by large storm events.

3 METHODOLOGY

3.1 Cross-Plot Analysis

A study of wireline SGR data was undertaken to determine whether the SGR signatures adequately differentiate rocks of different lithology and facies. If this were proven to be the case, it would warrant the time and cost involved in acquiring further SGR data from cores.

Wireline SGR data from Central Yardarino 1 and Cliff Head 3 were displayed in cross-plots, with the x-axes of the plots representing potassium concentration, and the y-axes representing the ratio of thorium to uranium. These plots were assessed for clusters of data, which represent lithologically similar units. Polygons separating each cluster were drawn, and the data cluster inside each polygon was assigned a colour. This colour was then displayed on the GR wireline log from that same well.

3.2 Core Spectral Gamma Ray Data

Full-hole cores taken during drilling of petroleum wells in the northern Perth Basin were analysed for their SGR signatures using an Exploranium GR-256 Gamma Ray Spectrometer. The GR-256 is a hand-held tool that can be used to measure SGR signatures from outcrop and core. Four discrete spectral windows are measured by the GR-256 and these four windows are known as regions of interest (ROI). The ROIs are set so that they record emissions from the decay paths of potassium, thorium and uranium as well as the total gamma ray counts (Exploranium, unpublished). The apparatus is fitted with an internal ^{137}caesium isotope source that is used to automatically calibrate the unit before each reading. Effects due to temperature fluctuations and component aging are thus minimised (Exploranium, unpublished).

Cores with depths measured in imperial units were sampled at intervals of one foot, and cores measured in metric units were sampled at intervals of 25cm. Cores were not removed from their trays during gamma ray sampling (Fig. 3.1). The counting window of the SGR tool was set at 15 seconds, and the

readings for each depth point were manually recorded. Core SGR data were manually entered into Microsoft Excel spreadsheets, and data files for each well were generated.

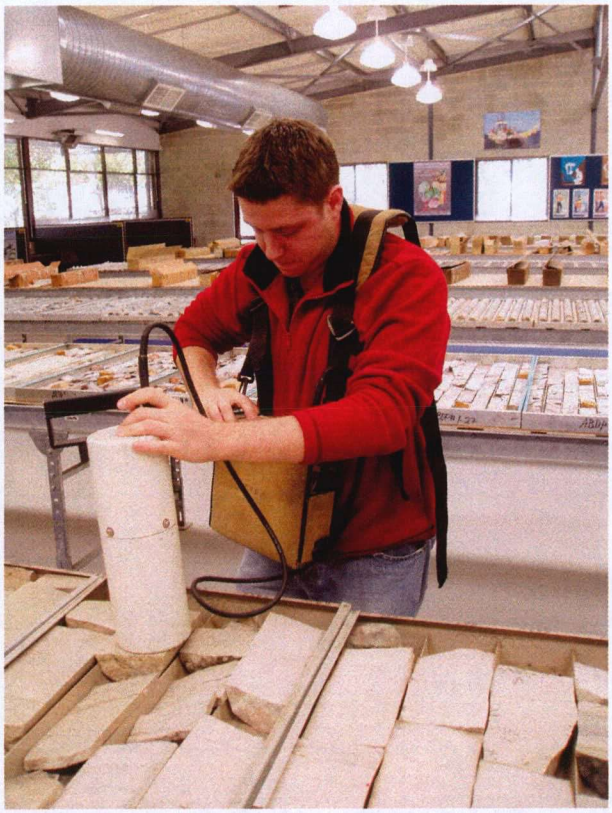

Figure 3.1 Acquisition of core spectral gamma ray data

3.2.1 Repeatability Study

A repeatability study was undertaken on three core rocktypes in order to determine and quantify the inherent errors of core gamma ray spectrometry. The study was conducted by gathering numerous readings from the same rocktype, and assessing how repeatable the data were as the duration of the counting window was altered. Three samples were measured 10 times each using counting windows of 10, 15, 30, and 60 seconds, and the four readings (K, Th, U and Total) were recorded. The standard deviations of the repeated measurements were plotted against the counting window. The rock samples analysed were sandstone, siltstone and mudstone, taken at depths of 10949.5, 11218.0 and 13411.5 ft respectively from Eneabba 1 drillcore (Fig. 3.2)

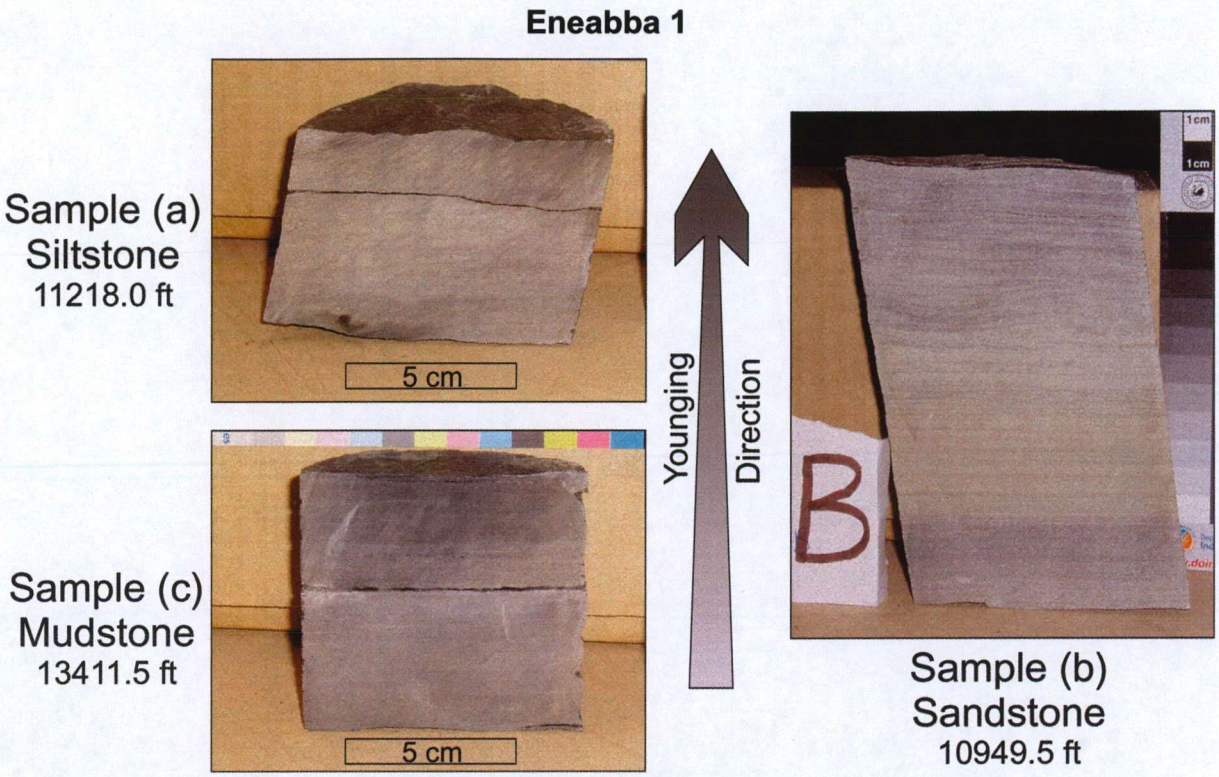

Figure 3.2 Rocktypes analysed as part of the repeatability study

3.3 Graphical Display of Spectral Gamma Ray Data

Petrolog Version 9.3.4 was the petrophysical software suite used in this study. This software was written by Crocker Data Processing Pty. Ltd., and was used to generate the composite SGR logs that can later be used for high-resolution facies correlation. The logs are briefly described here.

At each depth point, the relative potassium, thorium and uranium concentration (as derived from the spectral gamma ray emissions) are translated into a colour. This colour is then displayed as the infill of the total gamma ray curve. The Jingemia 1 composite SGR log is shown as an example (Fig. 3.3).

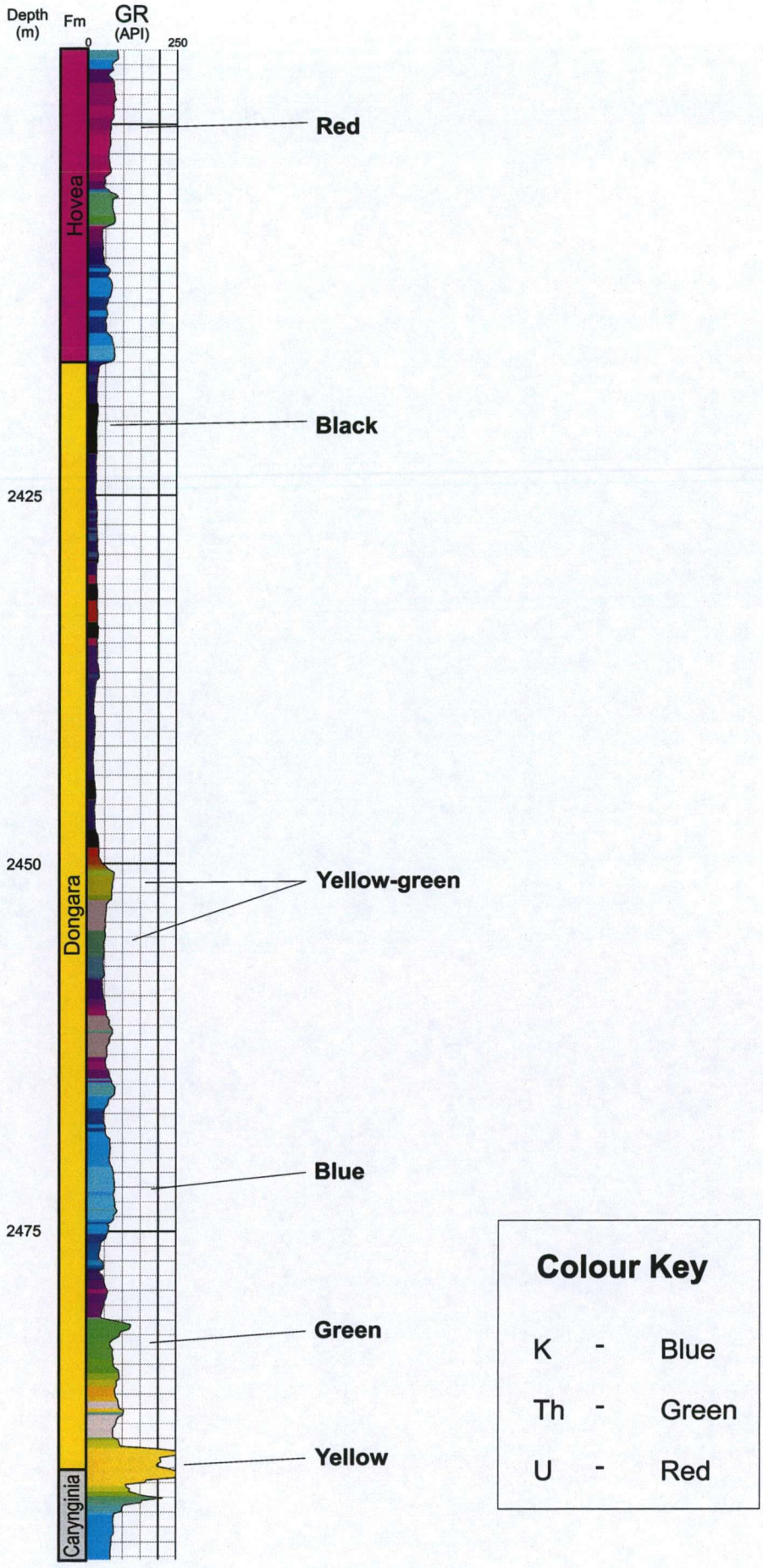

Figure 3.3 Jingemia 1 composite SGR log. Note that the infill colour changes in the logs are due to changing spectral gamma ray signature of the rocks.

Since the concentrations of K, Th and U are mineralogically dependent, mineralogical variations in rocktype are displayed as colour variations in these logs. Potassium is assigned the blue colour component, and uranium and thorium are assigned the red and green colour components respectively. For example, rocks that appear bright blue on the composite log are relatively concentrated in potassium, and hence could be interpreted as having appreciable amounts of K feldspar, illite or mica. These displays logs are particularly useful in areas where beds of different mineralogical character are indistinguishable on the basis of their total GR, but differences in their relative abundances of K, Th and U mean they are clearly discernible on the basis of their colour in a composite SGR plot. Examples of this can be seen in the Jingemia 1 SGR composite log (Fig. 3.3). Hence, these SGR composite logs have the potential to be used for high-resolution correlation and facies determination.

Each component (K, Th and U) has display limits that govern the intensity of the colour that is displayed on the composite log. These display limits are determined by calculating the 2.5th and 97.5th percentiles of each component's distribution. For example, below is a frequency distribution of the potassium reading from the SGR dataset of a hypothetical well (Fig. 3.4).

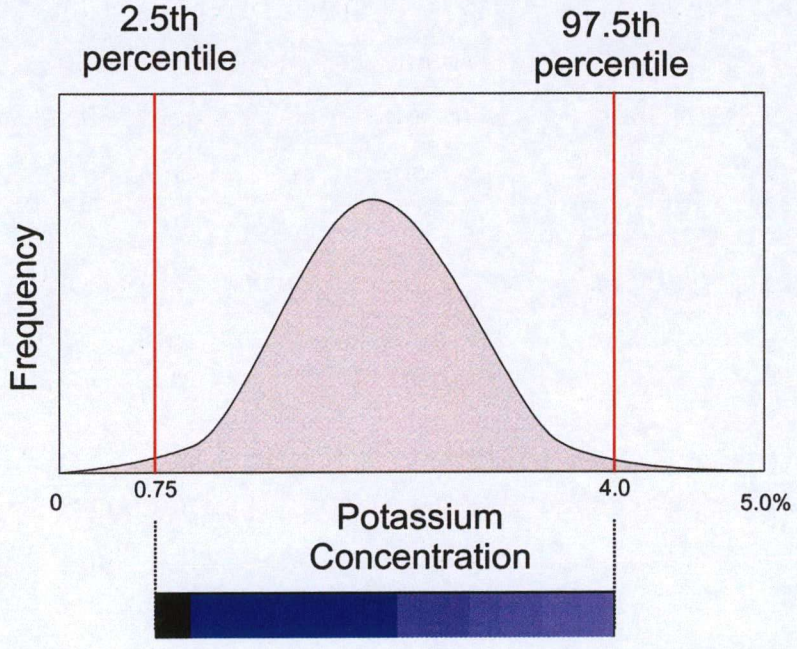

Figure 3.4. Example of a potassium histogram with display limits and their associated colours

Datapoints with the values less than or equal to the 2.5th percentile are displayed as black (zero intensity), and datapoints with values greater than or equal to the 97.5th percentile are displayed as bright blue (full intensity) on the SGR composite log (Fig. 3.4).

This same scaling procedure is used for three SGR components. Therefore, every depth point along the log has a K, Th and U value, and according to its position in the distribution within its dataset, has a certain colour intensity associated with it. The blending of the red, green and blue colours for each depth point creates a specific colour that is characteristic of the SGR signature. In the hypothetical situation that the sand at a particular depth is highly concentrated in all three components (K, Th and U), the potassium colour component would be bright blue, the thorium colour component would be bright red, and the thorium colour component would be bright green. The blending of full intensity blue, red and green produces white. Therefore the colour displayed on the composite log at this specific depth point would be white.

3.3.1 Core Spectral Gamma Ray Data

The frequency distribution from the entire core database was first collated in one continuous dataset. This was done only for the sole purpose of calculating the display limits for the whole core dataset.

Core SGR data from each well was then analysed separately using the Petrolog software, and composite SGR plots for each well were subsequently generated. These composite plots all contained the display limits that were set by the whole core dataset. These are the logs that are later used in high-resolution correlation.

3.3.2 Wireline Spectral Gamma Ray Data

The available wireline log SGR data was imported and displayed using the same petrophysical software as the core data. Identical SGR composite logs

were generated, however, the display limits were not fixed for all wells due a data bias in the wireline SGR datasets for the reasons explained below.

The wireline SGR log is generally run over the total depth extent of the well, while the cores are mainly only taken from the Dongara Sandstone reservoir unit. The K, Th and U distributions of the wireline SGR dataset would therefore differ from that of the core dataset. The Dongara Sandstone will influence the display limits of the core dataset, however, the wireline dataset will have display limits influenced by all formations. Wireline SGR composite logs therefore needed to have display limits set by the distribution of data from the Dongara Sandstone before the wireline and the core data could be compared. To do this, the display limits of the wireline SGR data were obtained from values only within the Dongara Sandstone interval. This process allows the wireline data to be displayed with the same bias that is inherent within the core data, so that these two datasets can be compared.

In addition, it was noticed that the wireline SGR data from one well was not comparable with wireline SGR data from another well, due to the data being acquired by different gamma ray tools, at different times and by different logging companies. As a result of these discrepancies, the display limits for the wireline SGR composite logs were defined on a well-by-well basis. Clare and Crowley (2001) claim that such an approach can minimise incompatibility issues between wells. From each well's full wireline SGR dataset, a new data subset was created which contained values only from the Dongara Sandstone. The display limits from this subset were calculated, and were used as the display limits when displaying the full dataset. This process was undertaken separately for all seven wells that contained wireline SGR data. Many of the wells containing wireline SGR data contained only a thin section of Dongara Sandstone. In such cases, relatively few data points were used to calculate the display limits which reduces the accuracy of scaling and therefore the consistency of the display colours between wells.

3.4 Stratigraphic Correlation

Palynological zonation data was the first step in unravelling the stratigraphy of the Dongara Sandstone. The *D. ericanus* and the *D. parvithola* palynological zones are of particular use in correlating the Dongara Sandstone, and these represent timezones within the Late Permian (Fig. 2.1). Very few wells in the northern Perth Basin have yielded palynology data within the Dongara Sandstone, and in many cases, those that do have poor vertical resolution. Nevertheless palynology data was used wherever possible, and was a helpful correlative tool. A facies correlation of was then derived within each palynological zone on the basis of the SGR signature (colours), and from this, palaeogeography distribution maps were generated.

The palaeogeography maps display topographically high areas during the Late Permian. The thickness of the Kockatea Shale can be used as an indicator of the palaeotopography at the time of marine transgression (Latest Permian – Earliest Triassic) (H. Young, pers. comm., 2004). Well control and seismic reflection data from both onshore and offshore were used by Voyager Energy to generate a Kockatea Shale isopach map. Crude indications of palaeotopographic highs are inferred where the shale thins. The palaeotopographic high areas from the Kockatea Shale isopach map were integrated into this study to constrain the palaeogeography maps of the Late Permian Dongara Sandstone.

4 RESULTS

4.1 Cross-Plot Results

Two distinct clusters of data were discerned in a cross-plot of SGR data from Central Yardarino 1 (Fig. 4.1). These clusters represented quartz-rich sands (yellow polygon) and fine-grained silts and shales (red and blue polygons). When these clusters are displayed on the total GR log, the Dongara Sandstone appeared consistent with pre-existing formation tops, and was clearly differentiated from the overlying and underlying sediments (Fig. 4.1). Cliff Head 3 SGR data also demonstrates this same trend, with sands (orange, yellow and green polygons) plotting to the left of the silts and shales (blue and grey polygons) (Fig. 4.2).

In general, SGR signatures for sandstone intervals were found to be consistently lower in potassium than the silts and shales. In addition, the High Cliff and Dongara Sandstones display substantial variability in the thorium/uranium ratio. On further inspection, it was discovered that the variability in the thorium/uranium ratio adequately differentiated radioactively 'hot' and 'cold' sands. For instance, in figure 4.3, the sandstones falling within the green and pink polygons (high values of Th to U) generally also have high total GR values, whilst sandstones falling in the blue polygon (lower values of Th to U) generally have a low total GR reading (Fig. 4.3).

Data from within the silt-shale polygons also showed variability in the thorium/uranium ratio. For Central Yardarino 1 (Fig 4.1), elevated thorium/uranium ratios clearly differentiate the Hovea Member (red polygon) from the lower thorium/uranium ratios observed within the Kockatea Shale and the Carynginia Formation (blue polygon). In Cliff Head 3 (Fig 4.2), the Irwin River Coal Measures (orange polygon) consistently showed the lowest concentrations of potassium, and had little variation in the thorium/uranium ratio. This meant that data from the Irwin River Coal Measures populate a separate cluster on their own.

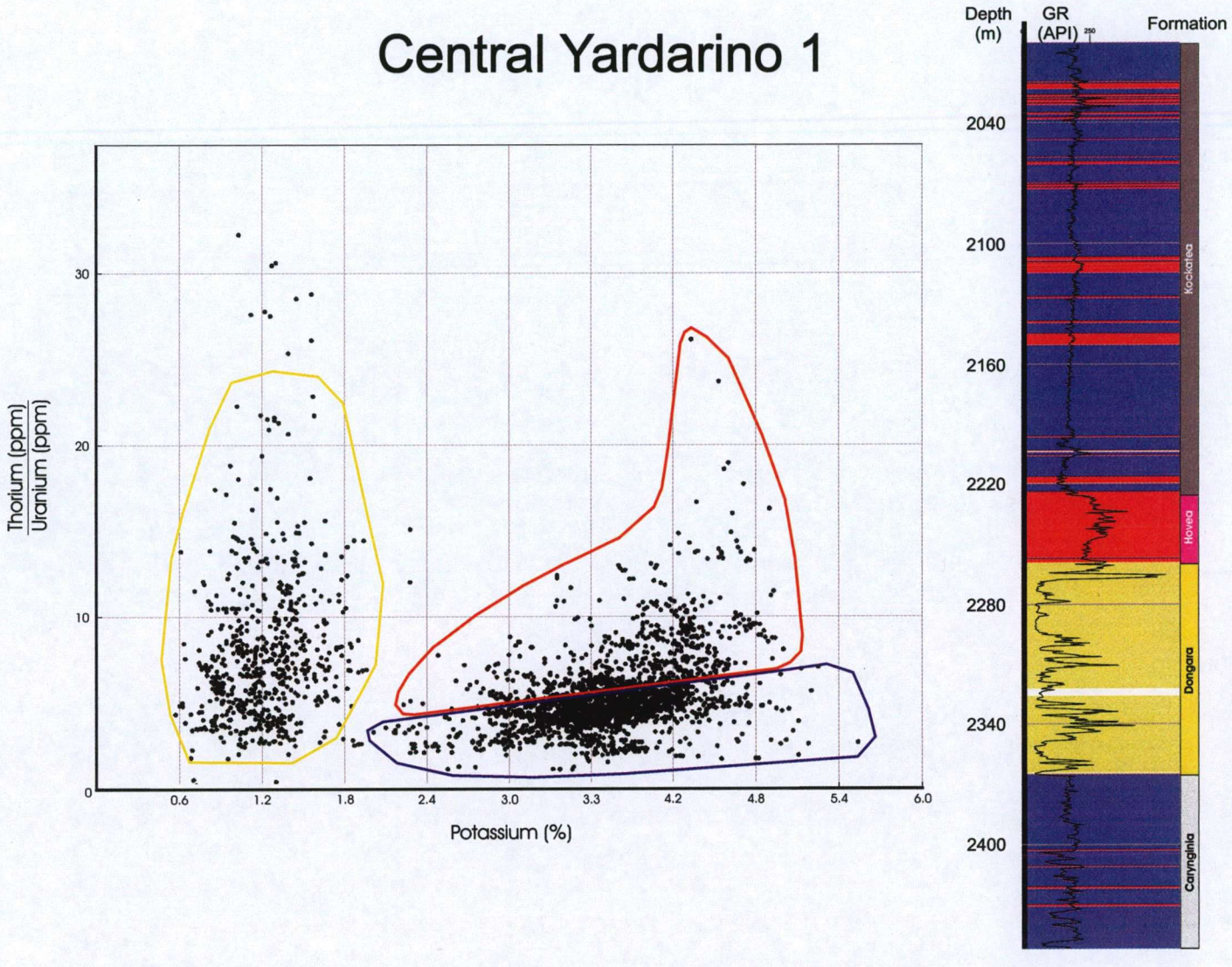

Figure 4.1 Central Yardarino 1 cross-plot of potassium vs. thorium/uranium wireline log data. Note that the data from silts and shales (red and blue polygons) can be easily differentiated from the sands (yellow polygon).

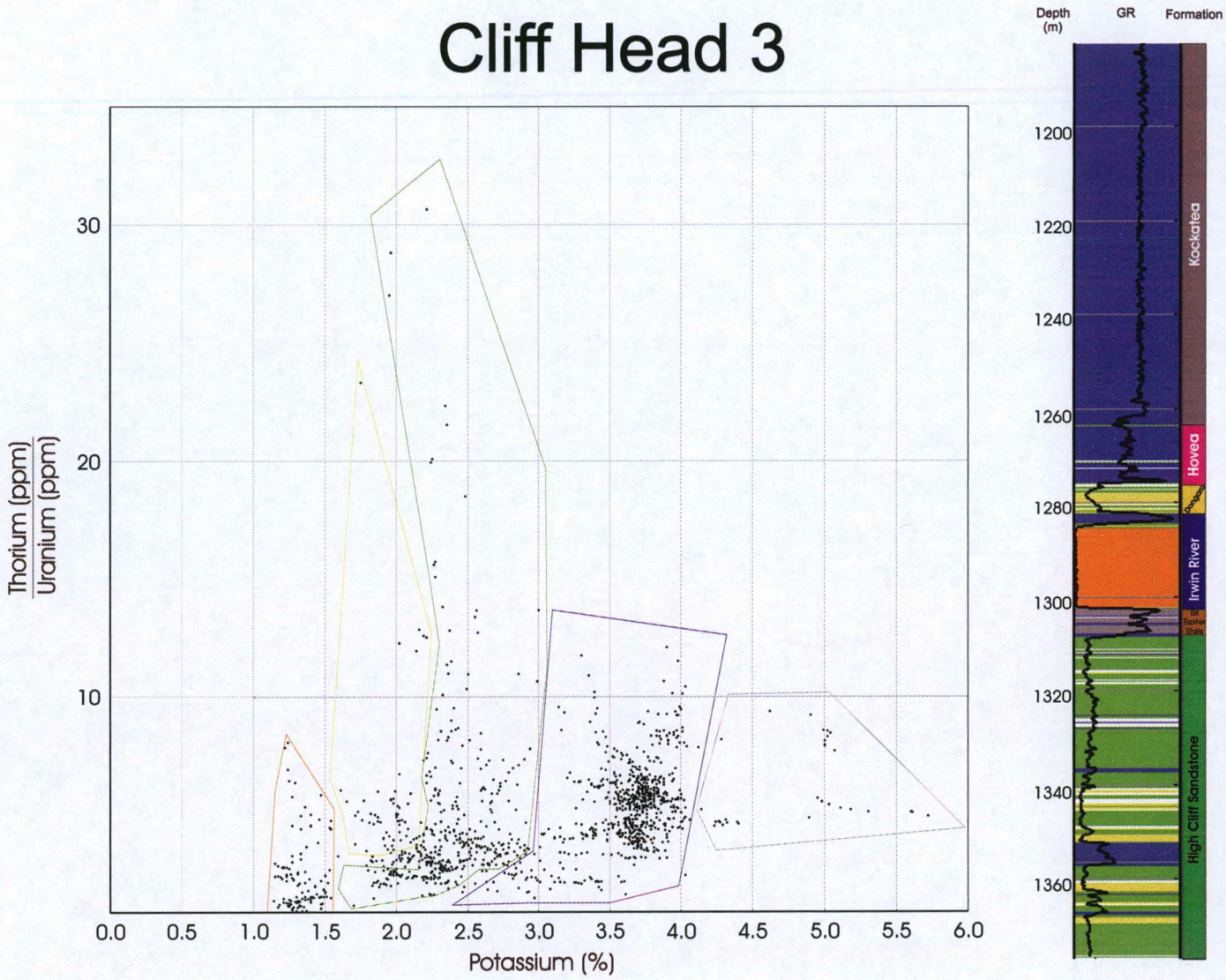

Figure 4.2 Cliff Head 3 cross-plot of potassium vs. thorium/uranium wireline log data. Note the sands (orange, yellow and green polygons) plot to the left of the silts and shales (blue and grey polygons)

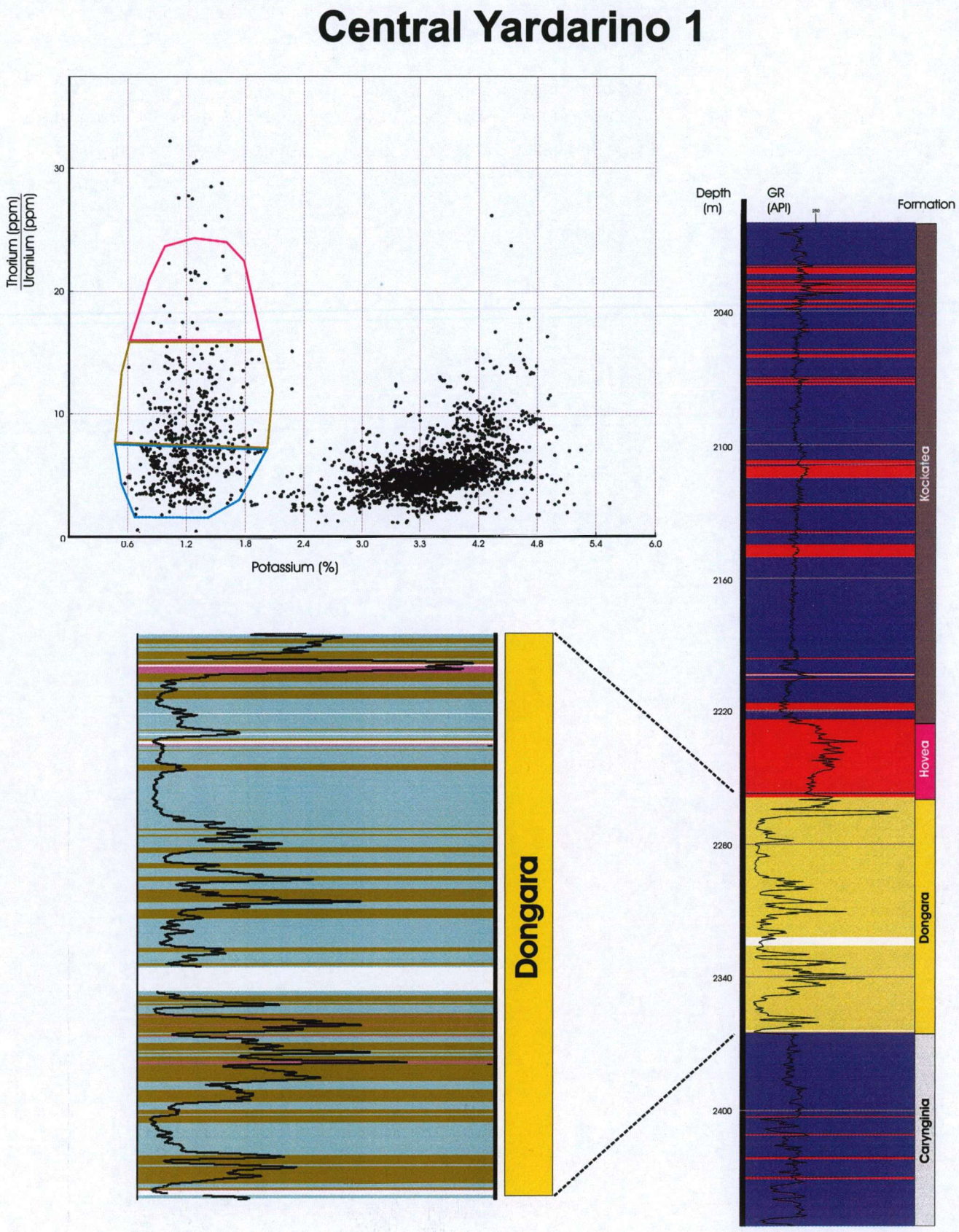

Figure 4.3 Central Yardarino 1 cross-plot of potassium vs. thorium/uranium. Note that data with high values of thorium/uranium plot in the high gamma ray intervals of the Dongara Sandstone.

Therefore, these sediments could be confidently differentiated from both the 'hot' and 'cold' intervals of the High Cliff and Dongara Sandstones. The High Cliff Sandstone and the Dongara Sandstone have very similar SGR signatures, and this can be seen by the overlap in the Cliff Head 3 cross-plot (Fig 4.2). There is a weak trend in the data showing that the High Cliff Sandstone is slightly elevated in potassium when compared to the Dongara Sandstone. However, the difference is not substantial enough to conclusively demonstrate two distinct populations of data.

4.2 Core Spectral Gamma Ray Results

Wells from the Perth Basin generally contain only one length of core (30ft) in the reservoir unit. Information regarding the whole reservoir unit of a particular well is therefore generally unavailable, especially when drilling difficulties are encountered and core recovery is not 100%. In such cases, the application and inclusion of these data into any facies correlation was limited.

Over 2600 SGR readings were taken from cores of Perth Basin sediments. For each well, the vertical extent of the cored interval, along with the number of SGR readings per core are annotated in Table 4.1. A core rating is also assigned to each core. This rating is a measure of how suitable the core data is for application in facies correlations. Low core ratings are given to cores that do not adequately represent the whole reservoir interval of that well (i.e. poor core recovery). On the other hand, fully cored Dongara Sandstone intervals, such as in Jingemia 4, were given a core rating of excellent. On rare occasions, core SGR data for whole core intervals appeared spurious. Such data were encountered in Hovea 3 and Cliff Head 3. In both situations, core SGR data did not reflect the wireline SGR equivalent. These two wells were excluded from facies correlations.

Table 4.1 List and description of core data gathered for this study

Well Name	Cored interval		Sample interval	Core Rating	Comments	No of SGR readings taken from core
	Min Depth	Max Depth				
Batavia 1	2794	2801.5	25 cm	☆	Poor reservoir coverage	32
Beekeeper 1	2781	2826	25 cm	☆	Poor reservoir coverage	85
Cent. Yardarino 1	2263	2281.5	25 cm	☆☆	Good reservoir coverage	75
Cliff Head 3	1278.25	1309	25 cm	×	Bad core SGR data	125
Dongara 1	5482	5633	1 ft	☆	Poor reservoir coverage	41
Dongara 4	5450.2	5670.5	1 ft	☆☆☆	Excellent reservoir coverage	328
Dongara 11	5529	5686	1 ft	☆☆☆	Excellent reservoir coverage	115
Dongara 12	5340	5614	1 ft	☆☆	Good reservoir coverage	106
Dongara 24	1460	1643	25 cm	☆☆	Good reservoir coverage	239
Hovea 3	1968.75	2049.75	25 cm	×	Bad core SGR data	325
Jingemia 4	2400	2482	25 cm	☆☆☆	Excellent reservoir coverage	338
Lockyer 1	3195	3209	25 cm	☆	Poor reservoir coverage	67
Mondarra 1	6687	10050	1 ft	×	Very poor reservoir coverage	24
Mondarra 2	8982	9022	1 ft	☆	Poor reservoir coverage	41
Mondarra 3	9303	9551	1 ft	☆	Poor reservoir coverage	61
Mt Horner 1	4588	7386	1 ft	☆	Poor reservoir coverage	35
Mt Horner 7	1232.5	1794.75	25 cm	☆☆	Good reservoir coverage	68
Nth Erregulla 1	9183	10581	1 ft	×	Very poor reservoir coverage	94
Strawberry Hill 1	8977	8992	1 ft	×	Very poor reservoir coverage	16
W. White Point 1	7156	7158.5	0.5 ft	×	Very poor reservoir coverage	6
Woodada 14	2175	2193.75	25 cm	×	Carbonate reservoir	34
Yardarino 1	6373	7787	1 ft	☆☆	Good reservoir coverage	143
Yardarino 2	7509	9931	1 ft	☆☆	Good reservoir coverage	336
					TOTAL	**2734**

× - Unusable core data
☆ - Poor reservoir coverage
☆☆ - Good reservoir coverage
☆☆☆ - Excellent reservoir coverage

4.2.1 Repeatability Study and the Determination of the Counting Window

The precision of SGR data is limited by the amount of time the detector is left to record natural gamma emissions. This counting window was decided upon by balancing the results of the repeatability study with the time and budgetary constraints.

The repeatability study quantified the inherent errors embedded in the data from each ROI (K, Th, U, Total). The thorium and uranium components displayed the greatest variability, with standard deviations of 4.0 and 1.4ppm respectively for a counting window of 15 seconds (Fig. 4.4). Potassium and Total GR have standard deviations that are quite low, only reading 0.25ppm and 0.6 respectively.

The standard deviations of the thorium and uranium repeatability data appear significant, reducing the confidence given to the core SGR data. However, the standard deviation values are thought by the author to be poorly constrained. This uncertainty is the result of calculating a standard deviation from a population too small to be statistically significant (i.e. population is too small to be representative of a gaussian distribution). One method to overcome this uncertainty is to use a greater number of readings in the standard deviation calculation. Due to time and budgetary limitations, this was not considered feasible, and 10 readings per sample was deemed adequate. Pragmatism also played a large part in assigning the counting window, since the SGR data from core need only be as precise as its wireline equivalent. The limitations of the wireline SGR data are described in the discussion chapter. For a counting window of 15 seconds, the embedded errors appear to be substantial (especially in the thorium concentrations), however, taking into account the degree of accuracy required for this study, and the fact that core SGR data could confidently be compared to wireline SGR data (Fig. 4.5), the core SGR data were considered to be sufficiently accurate.

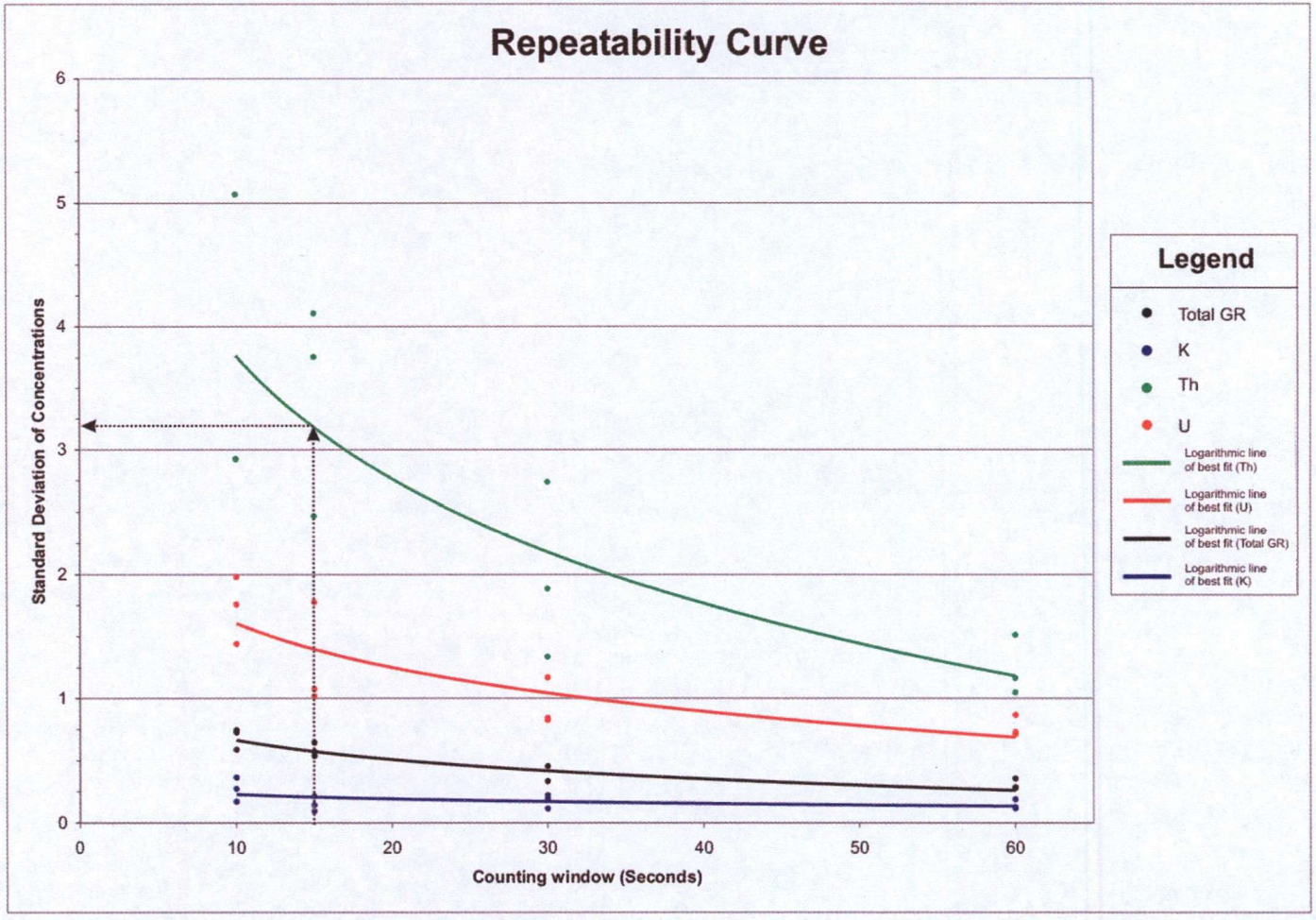

Figure 4.4 Repeatability curve, displaying the inherent variation in the core spectral gamma ray logging technique as a function of the counting window. Note that the data becomes more repeatable (standard deviation decreases) as the counting window increases

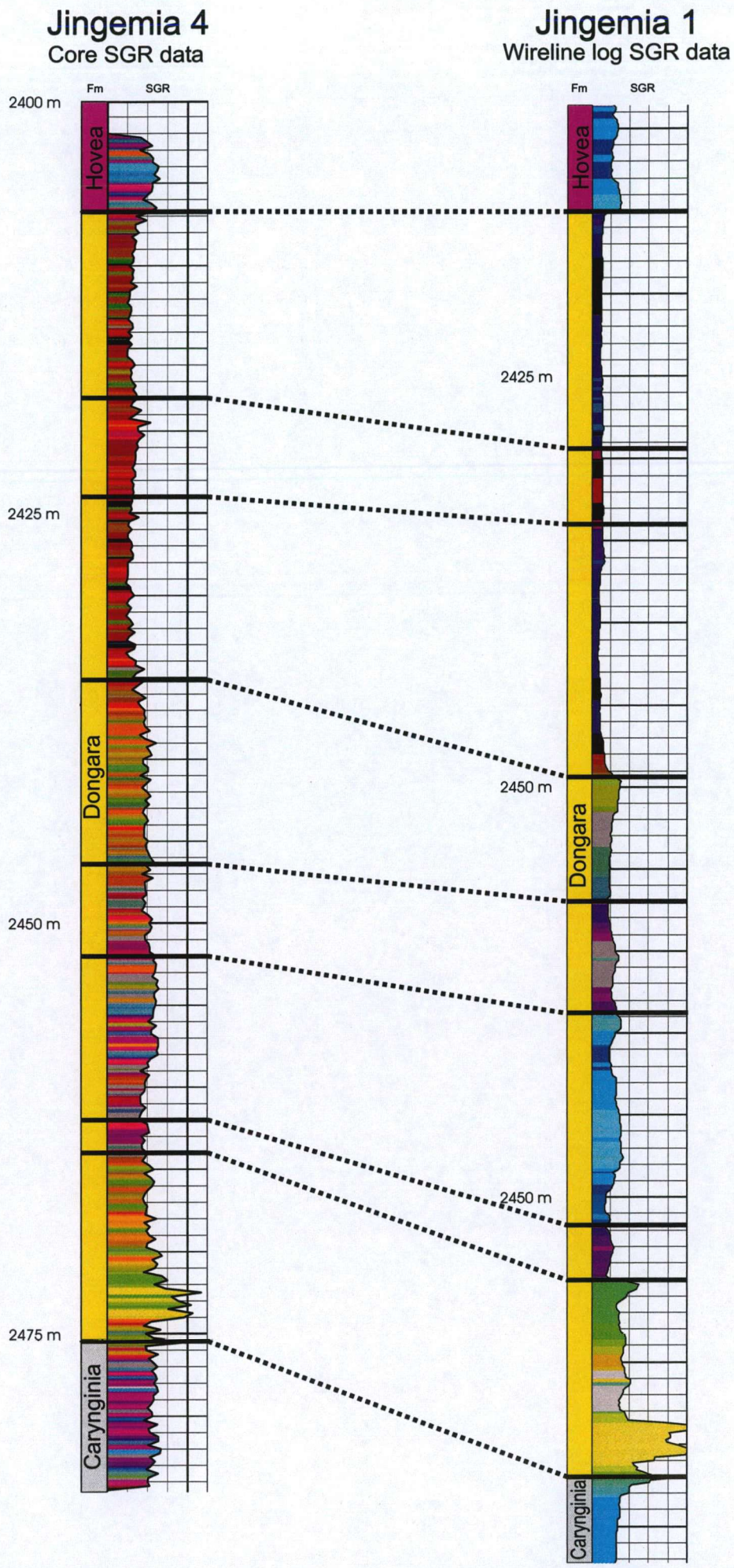

Figure 4.5 Jingemia 1 and Jingemia 4 SGR composite logs. Note the similarities between the spectral gamma ray signatures of the core SGR log (Jingemia 4) and the wireline SGR log (Jingemia 1)

4.3 Spectral Gamma Ray Composite Logs

4.3.1 Core Spectral Gamma Ray Data Results

Histograms from a dataset containing all the core SGR data are annotated in the appendix, and these were used to assign the display limits of all the core SGR data on the composite logs. The limits (as discussed previously) are defined as the 2.5th and 97.5th percentiles of the whole dataset for each element. The limits selected are given in Table 4.2.

Table 4.2. Display limits determined from the 2.5th and 97.5th percentiles from the frequency distribution for the entire core SGR dataset

Element		2.5th percentile	97.5th percentile
K	(%)	0.60	2.33
U	(ppm)	1.02	8.12
Th	(ppm)	5.15	24.23

Spectral gamma ray data from cores can clearly discern mineralogically different beds when viewed as composite SGR logs. Colour variations in the composite logs are consistent with changes in wireline gamma ray intensity and variations in grainsize (Fig. 4.6). This proves that core SGR data is effective in differentiating intra-formational character of the Dongara Sandstone, and thus may have applications for facies correlation.

4.3.2 Wireline Spectral Gamma Ray Results

Wireline SGR data was available for seven wells within the study area, however, only three of these could be confidently used in facies correlation. The four wells rejected were located in areas where the Dongara Sandstone is relatively thin, and little to no intra-formational variations were present. These wells were Cliff Head 3, Mentelle 1, Twin Lions 1 and Vindara 1. The three remaining wells (Central Yardarino 1, Jingemia 1 and Mt Horner 7) encountered thick sections of Dongara Sandstone with clear intra-formational variation, and as such were the only wells that comprised the wireline SGR dataset. The colour variations seen in the Jingemia 1 composite log are indicators of such intra-formational character (Fig. 3.3)

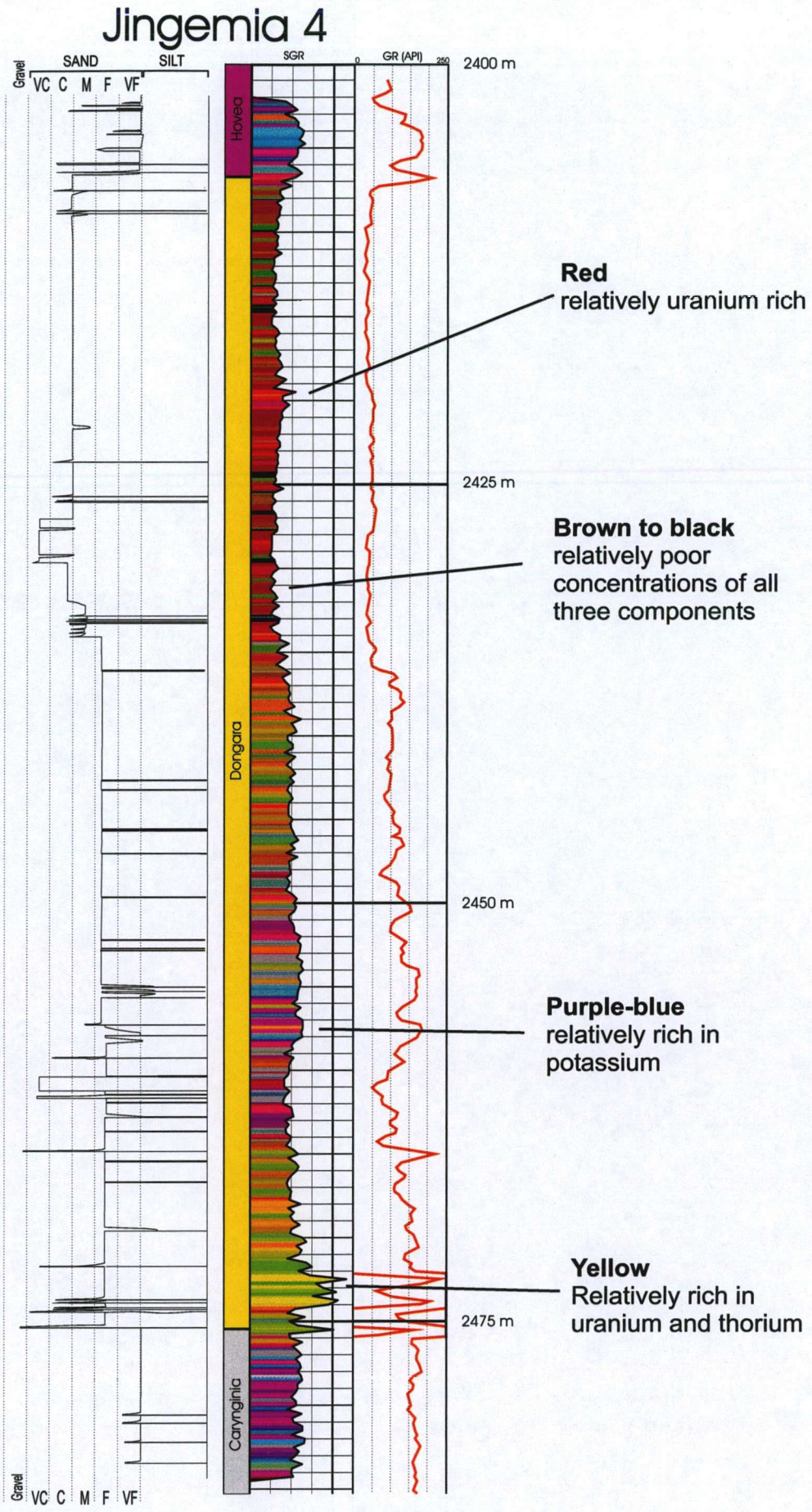

Figure 4.6 Jingemia 4 core SGR log and grainsize log.

It is important to note that:

The GR intensity from core spectrometry closely resembles the GR intensity from the wireline GR log

The GR intensity varies consistently with the grainsize

There is substantial variation in the colours of the composite log within the fine sand section of the reservoir.

5 DISCUSSION

5.1 Comparison of Core and Wireline Spectral Gamma Ray Results

Total gamma ray readings from core gave confident results, and could be easily matched to the total GR log in wells where there was appreciable lengths of core (Fig. 4.6). Total GR values from the cores are consistently lower than their wireline equivalent, but this can be expected due to the differing sample volumes of each technique. There was, however, a consistency in the shape of the GR logs between both techniques, and this was extremely useful when applying core shifts (Fig. 4.6).

After calculating the display limits for each well individually (as described in the methodology section), clear comparisons between the wireline and the core SGR data can be made. The colours displayed in the Jingemia 4 core SGR composite log were very strongly correlated to the Jingemia 1 wireline SGR composite log (Fig. 4.5). Between wells Jingemia 1 and Jingemia 4, equivalent sediment intervals commonly displayed similar colours (Fig. 4.5). This indicates that the core and wireline SGR signatures are very similar, even though the methods for acquiring these two types of data differ drastically.

Therefore, it can be concluded that:

1) The core SGR data is sufficiently precise.
2) The core SGR data can be confidently compared with wireline SGR data from wells in the same field.
3) Core SGR data is an effective substitute for wireline SGR data if the cored interval is of sufficient length.

It is also noted that the core SGR composite logs commonly appear substantially more jagged or banded than the wireline SGR data. This is due to the inherent differences in the two SGR data acquisition methodologies. Because wireline SGR is acquired from a moving receiver, the data appears more smoothed. This is opposed to outcrop and core spectrometry where the receiver is maintained stationary during each spot reading.

5.2 Suitability of Spectral Gamma Ray as a High-Resolution Correlation Tool

The cross-plot analysis was a valuable step in determining the suitability of SGR data as a lithology discriminator. The cross-plots displayed clusters of data that separated out the major lithotypes (i.e. sand and silt/shale), but more importantly, they also discriminated intra-formational populations. In particular, data from the Dongara Sandstone showed that variation in the thorium/uranium ratio separated out radioactively 'hot' (monazite-rich) sands from sands that are radioactively 'cold' (monazite-poor). This therefore proves that not only can spectral gamma ray data differentiate sediments of different lithology, it can also highlight intra-formational character.

The ability of SGR data to discriminate intra-formational populations means that utilising SGR information can greatly boost confidence in subsurface correlation. Due to the nature of the 'hot' sands within the Dongara Sandstone, correlations based on total GR could potentially be erroneous. An example of both SGR and GR correlation between Dongara 11 and Yardarino 1 is seen in Figure 5.1. It is noted that since mildly hot sands cannot be differentiated from shaly intervals, total GR will provide the wrong indications of lithology (Fig. 5.2). The application of the SGR tool can easily indicate which element is causing the gamma ray signature to be high, hence mineralogy and facies interpretations can be made. The utilisation of SGR data can therefore constrain new levels of correlation not possible using total GR data.

This has implications for the petroleum industry in the fact that greater confidence can be assigned to correlations when SGR data is used. Facies correlations can easily be made on the basis of SGR signature, particularly within the Dongara Sandstone. Improved facies correlation can better constrain the depositional environment of the Dongara Sandstone, and predictions on sand distribution and reservoir quality can therefore be made with greater confidence.

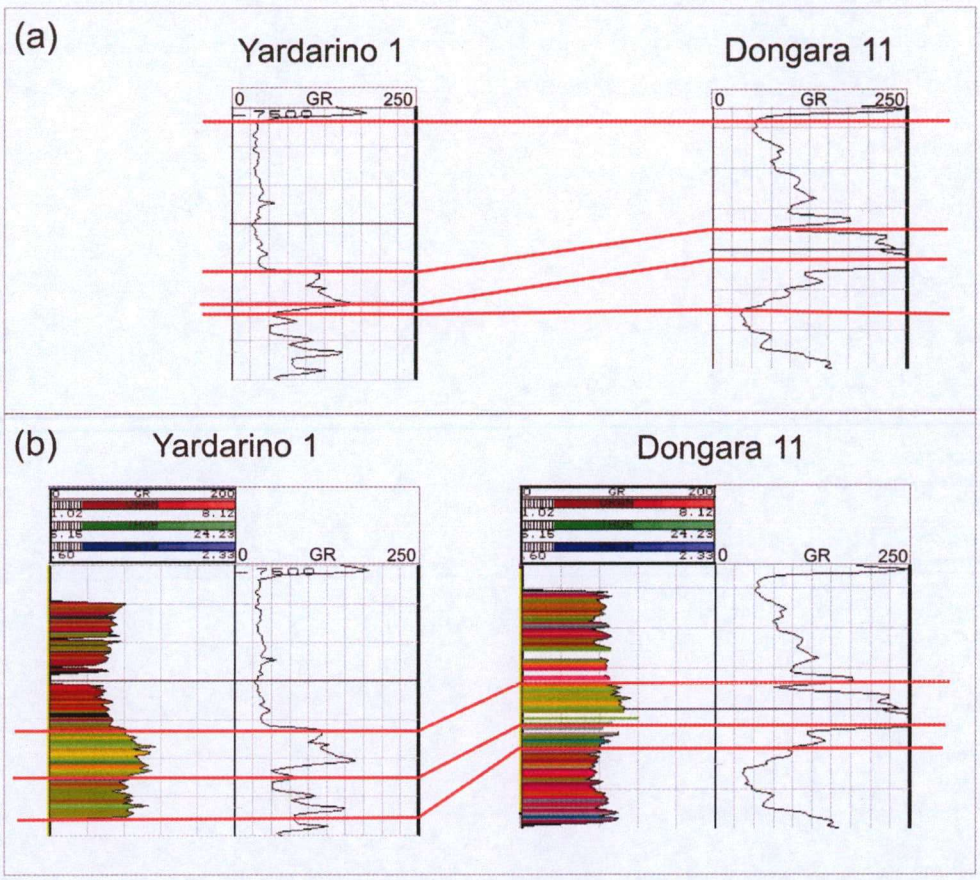

Figure 5.1 Correlations between wells Yardarino 1 and Dongara 11 based on GR character, and then based on SGR character. Note that correlation picks using the GR properties are slightly different to those same picks assigned on the SGR character.

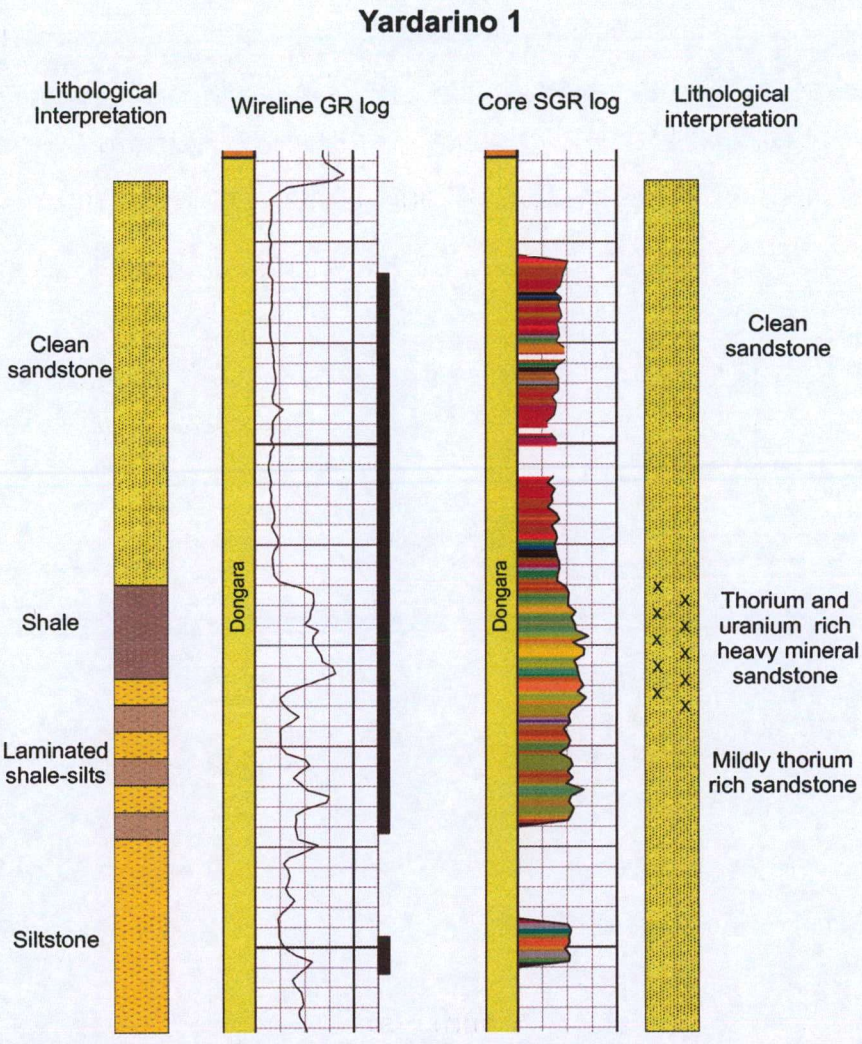

Figure 5.2 Indications of lithology using GR signature and SGR signatures. Note that intervals which appear shaly on the GR log, are in fact thorium-rich mildly hot sands when characterised by SGR data.

5.3 Limitations to Spectral Gamma Ray Analysis

5.3.1 Diagenetic Considerations

There have been many publications describing the changes in the SGR signature as a function of weathering and diagenesis, with applications mainly pertaining to soil mapping and palaeoclimatology studies (Wilford et al., 2001; Ruffell and Worden, 2000). The basis behind these studies is that K-feldspar and mica (minerals that contribute most to the potassium signature of crystalline rocks) are easily altered during diagenesis and weathering under humid conditions, and in some instances K is mobilised and removed from the system (Ruffell and Worden, 2000; Wilford et al., 2001). This leads to a depletion of K when compared to the relatively insoluble Th and U fractions, and can be a measurable feature of the SGR signature of the rock.

In petroleum related applications, K depletion is inferred to be a result of weathering at the sediment source, and is specifically excluded from post-depositional mechanisms. The alteration of feldspar and mica is common during burial diagenesis of arenites, however, it is commonly noted that feldspars and micas form authigenic clays under these conditions. Subsequently, there is no net loss of K from the system after deposition, and thus for the purposes of this study the author discounts the effect of diagenesis on the potassium gamma ray signature.

The thorium-rich units in this study are interpreted as sediments with high concentrations of the mineral monazite. Morton and Hallsworth (1999) demonstrate that monazite is stable under burial diagenesis. Grains from the North Sea recovered from burial depths of 4400m display no surface corrosion or etching when viewed under the scanning electron microscope (Fig. 5.3).

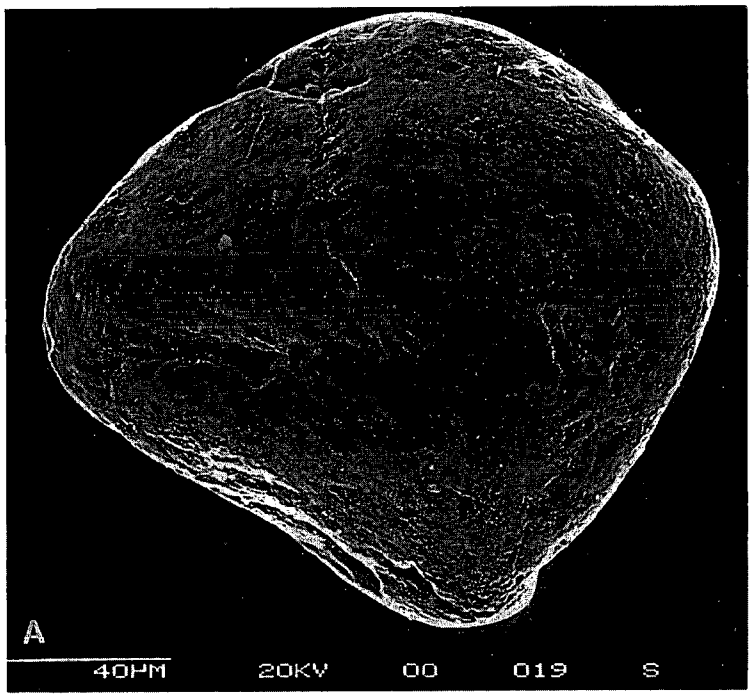

Figure 5.3 Scanning Electron Microscope image of a monazite grain recovered from a sandstone in the North Sea. Note the absence of etching or dissolution features on the surface of the mineral, indicating that the mineral has not been chemically altered. (from Morton and Hallsworth, 1999)

Diagenetic enrichment of thorium is only seen in rare earth element phosphates, and is argued by Hurst and Milodowski (1996) to be of rare occurrence, and even if present, would be overshadowed by detrital thorium concentrations. Therefore it can be concluded that, due to the above factors, diagenetic mechanisms, both dissolution and enrichment, are not considered to play a part in the thorium concentration of sandstones.

Uranium is quite mobile under oxidising conditions, where it is present in its uranyl form, U^{6+} (Adams and Weaver, 1958; Rider, 1996). Uranium in this oxidised form can be transported in water bodies; however, under reducing conditions, it reverts back to its insoluble form. This is thought to be the reason for the high concentration of uranium in black shales deposited under anoxic conditions. The presence and mechanisms of uranium deposition in sediments has been known for many years, and are outlined in Adams and Weaver (1958). During diagenesis, oxygenated pore water can re-mobilise uranium from the rock, and leach it from the system. If leaching has occurred, uranium depletion would be expected through permeable sections of sandstone, and tighter sandstone beds would demonstrate relatively higher uranium concentrations. The uranium wireline logs in this study indicate a relatively uniform uranium concentration throughout Dongara Sandstone intervals, therefore such leaching is not likely to have occurred during the diagenetic history of the Dongara Sandstone.

5.3.2 Limitations to Core Spectral Gamma Ray Analysis

The discrete effects of the sampling surface on outcrop gamma ray spectrometry are outlined in Svendsen and Hartley (2001), and are only briefly addressed here. The orientation of the gamma ray receiver with respect to the sampling rock face and bedding can spuriously increase or reduce the number of counts recorded (Fig. 5.4). Many of these effects are not applicable to core spectrometry, because the receiver orientation, bedding orientation and sampling environment were all maintained consistent throughout sampling (Fig. 3.1). The contamination effects from neighbouring

core in the core tray are considered to be minimal, considering a majority of the recorded gamma rays emanate from rocks directly below the receiver (Fig. 5.4). In addition, instrumental effects are not considered here to influence the precision of the core SGR data, because all core data was recorded by the same instrument, at the same time, and under the same environmental conditions.

Sidewall cores are more commonly taken throughout the whole reservoir interval, and would provide greater information about the total reservoir unit. However, due to the small sample size, sidewall cores are not considered to yield sensible data when using the same spectrometry technique as for the full-hole cores.

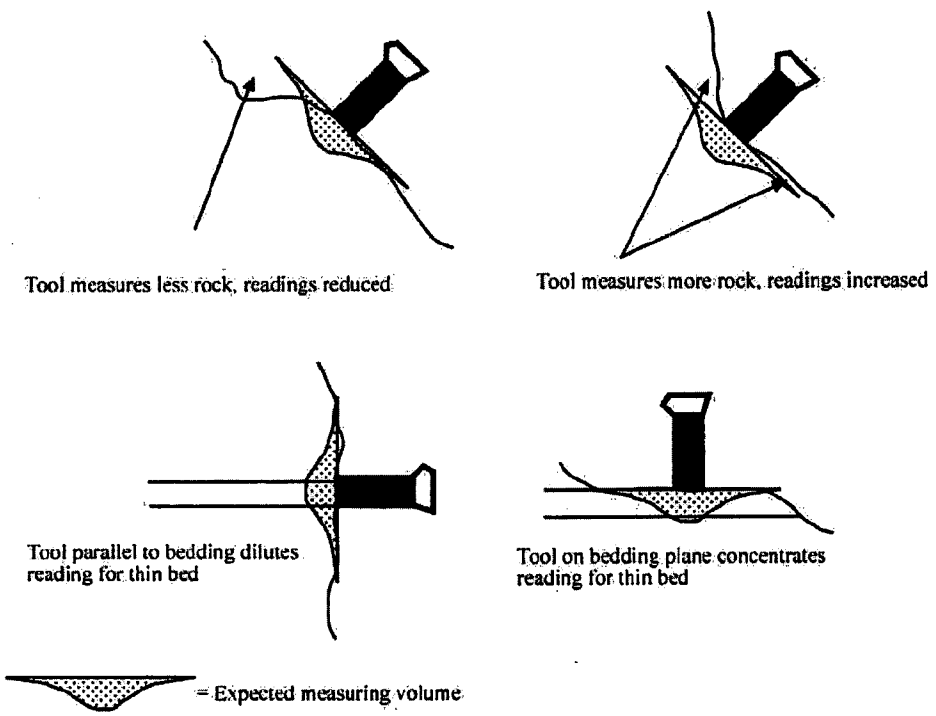

Figure 5.4 The effects that receiver orientation has on outcrop SGR sampling. Note that the measuring volume is contained mostly below the receiver. Diagram from Svendsen and Hartley, 2001

5.3.3 Limitations to Wireline Spectral Gamma Ray Analysis

Downhole SGR data is recorded in the borehole while the receiver is pulled up through the hole. In the downhole environment, there are specific factors that can affect the SGR reading, such as well casing, drilling mud additives, and washed-out borehole conditions (Rider, 1996).

The counting times of wireline SGR data are generally shorter than the counting times in outcrop spectrometry. The wireline tool records emissions at *c.*15cm intervals as the receiver is being pulled up the borehole (Rider, 1996). This generally means that the wireline gamma ray data is averaged in a vertical sense (Davies and Elliott, 1995). This has the greatest effect on data from components that emit only relatively few gamma emissions (thorium and uranium).

Potassium chloride (KCl) is a common additive in drilling fluid, and due to its potassium content, spuriously raises the potassium gamma ray response. This effect is easily accounted for, and is usually corrected by the logging company soon after the wireline logs are run (Baker Atlas, 1992).

Poor borehole conditions are known to affect the GR logs, especially where attenuation (Compton scattering) occurs in the high-density mud accumulations of washed-out zones (Rider, 1996). The interval of interest in this study is the Dongara Sandstone, which is known to be stable in the borehole environment and is not prone to washout. This mechanism is therefore not considered important in this study.

Borehole casing has a noticeable attenuation effect on the gamma ray response. This attenuation can be crudely accounted for with simple formulae annotated in many logging manuals (Baker Atlas, 1992). Casing is commonly placed in the overburden intervals, and as such, the gamma ray response of these units can be attenuated. The Dongara Sandstone was not cased in any of the exploration wells that contained wireline spectral gamma ray data, therefore attenuation is not considered to affect this study.

Minor well-specific effects are still accounted for by the process outlined in the methodology of wireline analysis (section 3.3.2). The display limits for wireline SGR composite log plots are set on basis of the distribution of each well's spectral dataset. Clare and Crowley (2001) argue that this well-by-well approach minimises the effects of KCl-enriched drilling muds and other such well-specific effects.

6 EXAMPLE APPLICATION OF SPECTRAL GAMMA RAY CORRELATION

A detailed sequence stratigraphic correlation of the Dongara Sandstone across the northern Perth Basin is beyond the scope for this study. However, in order to demonstrate the applicability and usefulness of SGR data as a tool to aid high-resolution correlation, a brief correlation of the thorium-rich sands to determine the distribution of depositional environments has been undertaken.

6.1 Facies Correlations for Palaeogeographic Mapping

A facies correlation of the thorium-rich hot sands was used to constrain palaeogeographic interpretations by mapping out sediments in which heavy minerals (namely monazite) are concentrated. Upon careful correlation of these sands, two distinct areas of monazite concentrations were identified. These were interpreted as beaches, and indicate the palaeo-shorelines of chronologically separate sediment packages (Figs 6.1 and 6.2). These claims are supported by the presence of beach specific sedimentary structures in corresponding cores, such as planar cross-bedding and gravelly to conglomeratic lenses. These shorelines could be used as facies anchors when constructing palaeofacies maps for the Late Permian.

The palynological zonation of the Dongara Sandstone provides the primary chronostratigraphic subdivision, however, the SGR data suggest two separate sediment packages within the *D. ericanus* sequence, and one in the overlying *D. parvithola* sediments. These three sediment packages and their associated beaches are named *D. ericanus 1*, *D. ericanus 2* and *D. parvithola* respectively for the purposes of this study and are described in detail below.

6.1.1 *D. ericanus* Sediment Package 1

The beach and its associated proximal shoreface deposits for this sediment package are best defined in the wells Jingemia 1 and 4 (Fig. 6.3). The beach runs roughly east-west, and can be correlated eastward in the wireline GR logs of neighbouring wells (Fig 6.1). This beach is thought to extend east of Mondarra 2, however, due to lack of well control, the precise extent is uncertain. The interpreted palaeogeography for this time interval is shown in Figure 6.1

These deposits are interpreted as a lowstand sediment package, deposited in the early stages of the late Permian. The incised channels feeding sediments into these beaches are thought to be represented in the low total GR signature sands intersected at the base of Yardarino 2 (Fig. 6.3).

6.1.2 *D. ericanus* Sediment Package 2

The second beach in the *D. ericanus* palynozone is wider than the first beach (Fig. 6.2). This could possibly be the result of high frequency eustatic variations on a shallow dipping marine shelf. This beach runs roughly NE-SW between the Yardarino and Dongara fields. Wireline total GR logs of Illyarrie 1 and Dongara 27 demonstrated high gamma ray intervals, and these were helpful in defining the lateral extent of this beach facies. The distribution of this beach facies is congruent with the interpreted palaeo-highs (Fig. 6.2). Beach facies are laterally proximal to the nearshore marine depositional facies in coastline environments, and as such, beach and nearshore marine sediments commonly appear together in the cores. Nearshore marine facies includes upper shoreface and lagoonal sediments, and are characterised by their grainsize and bioturbation structures present in core (Fig. 6.4). Owad-Jones and Ellis (2000) also interpret sections within the Dongara Sandstone in this area as to have been deposited in a beach environment. Cores from Mt Horner 7 display fluvial sedimentary structures (Fig. 6.5), and these channels are thought to have supplied the sediments that constitute the *D. ericanus* 2 beach.

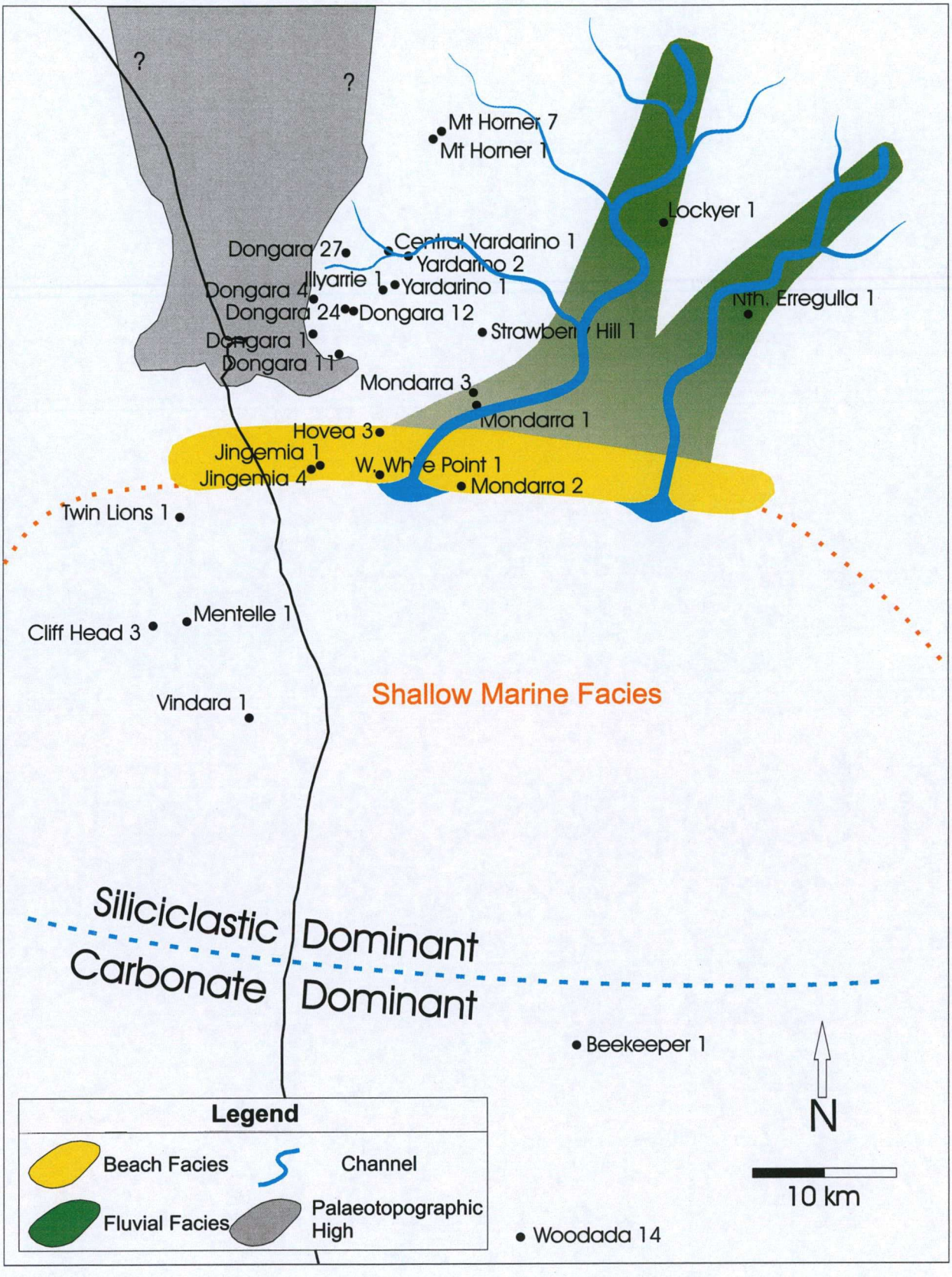

Figure 6.1 Palaeogeography of the *D. ericanus* 1 sediment package

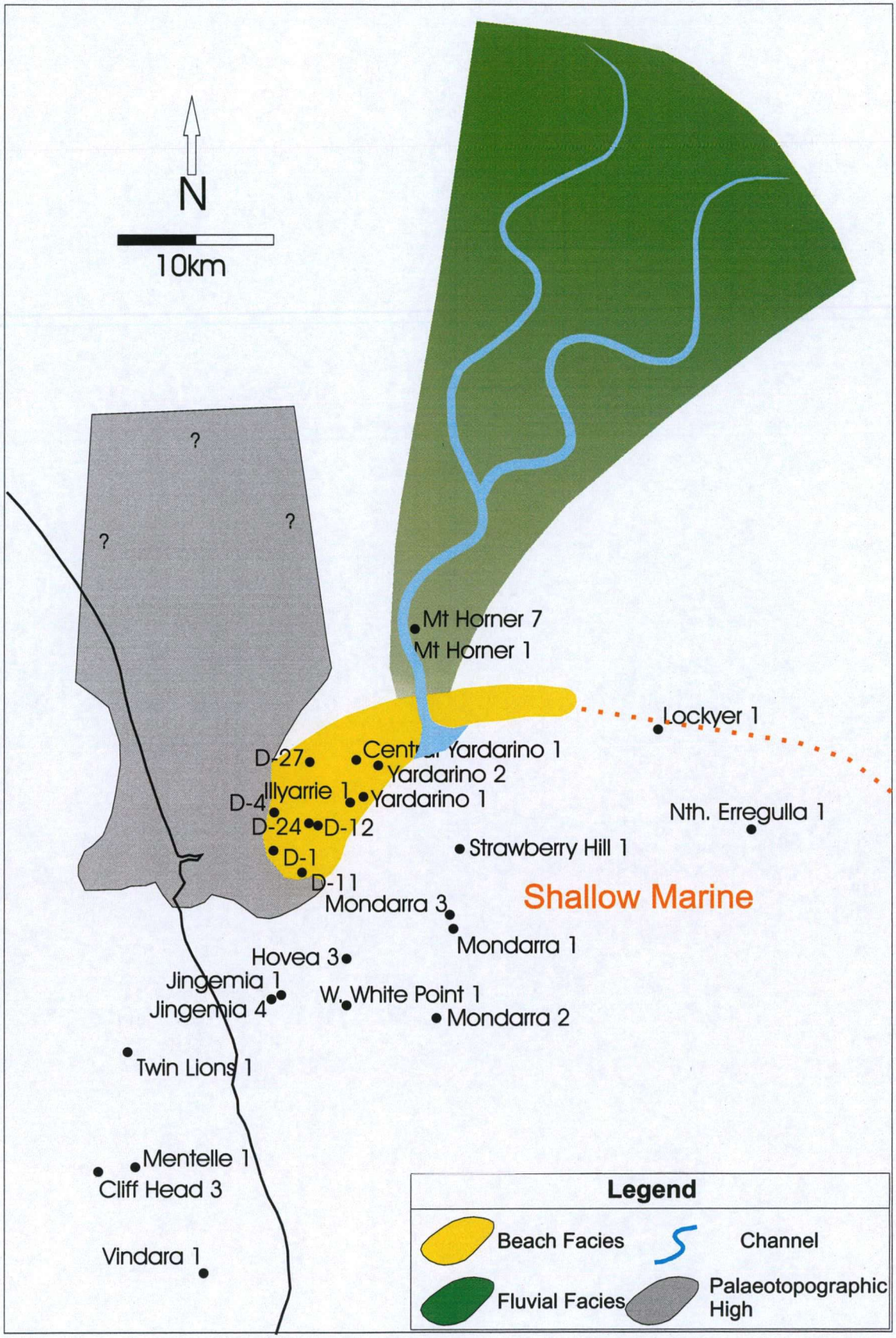

Figure 6.2 Palaeogeography of the *D. ericanus* 2 sediment package.

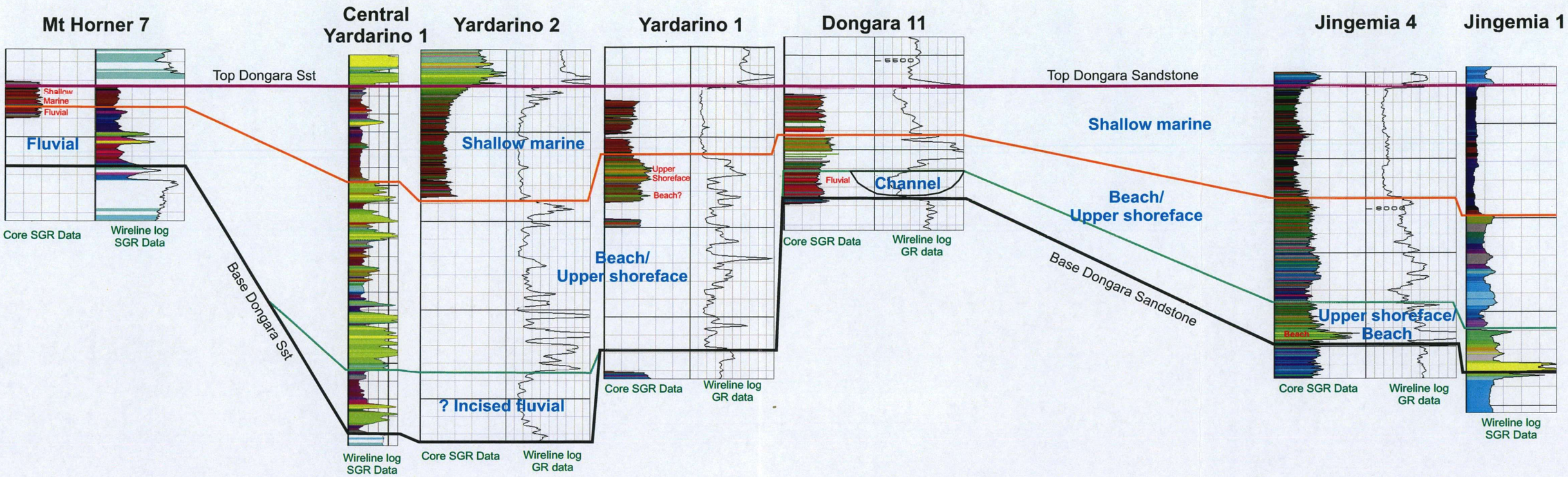

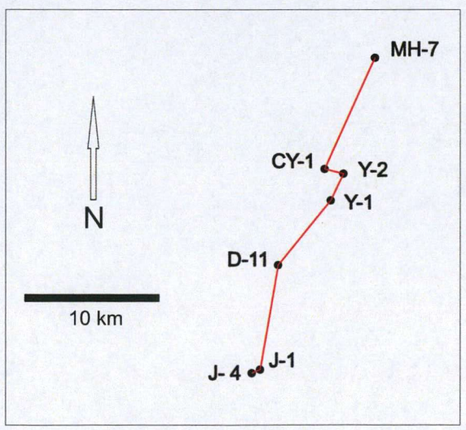

Legend

Wireline log GR data	Type of gamma ray data used in the log		Top *D.ericanus* 2 sequence
Fluvial	Palaeoenvironment from core structures		Top *D.ericanus* 1 sequence
Beach/ Upper shoreface	Facies Interpretation		Top *D.parvithola* sequence

Figure 6.3 Cross section through wells. Note that the facies interpretations are annotated

Nearshore Marine Sedimentary Structures

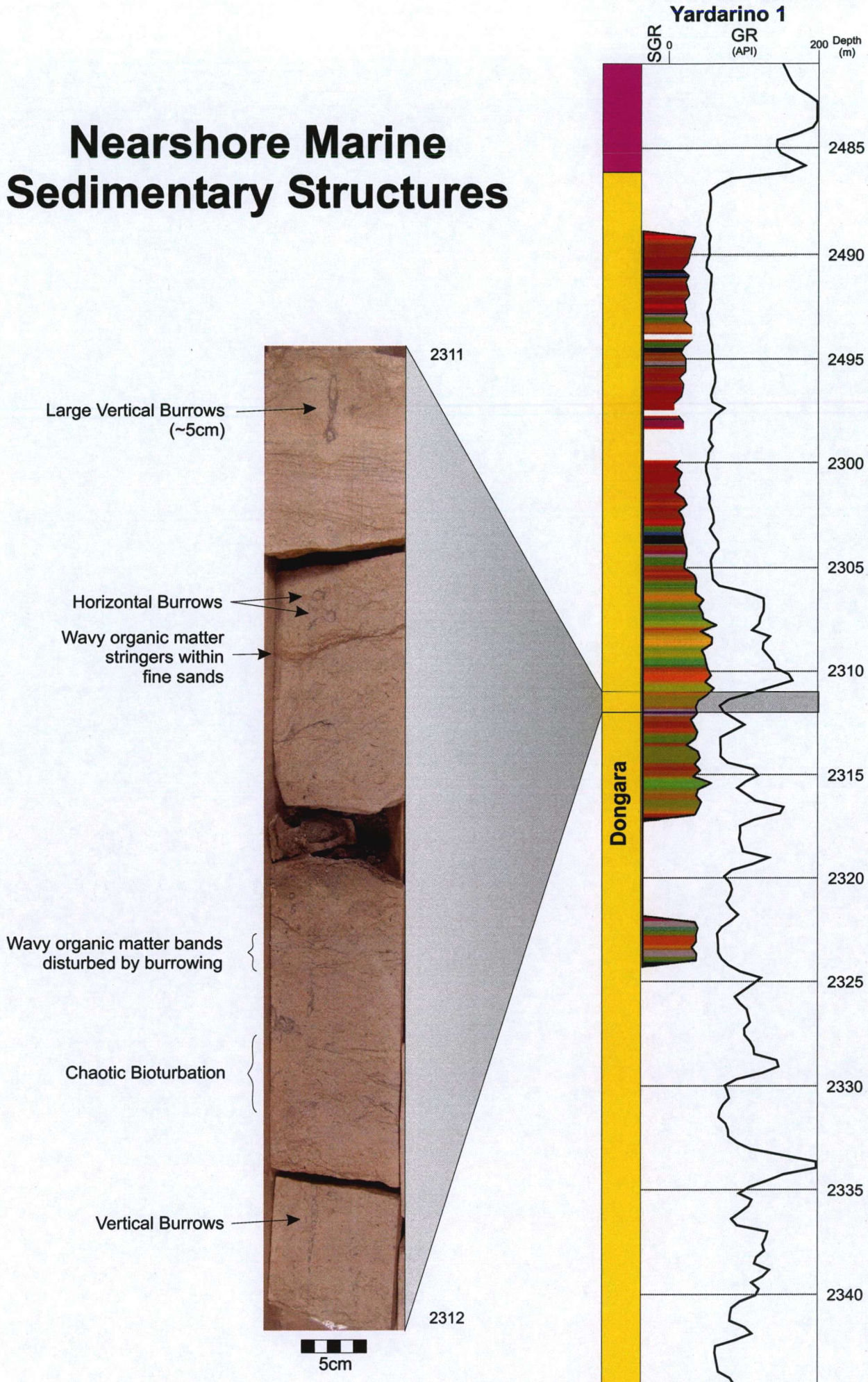

Figure 6.4 Typical nearshore marine (possibly lagoonal) sedimentary structures, as demonstrated in core from Central Yardarino 1.

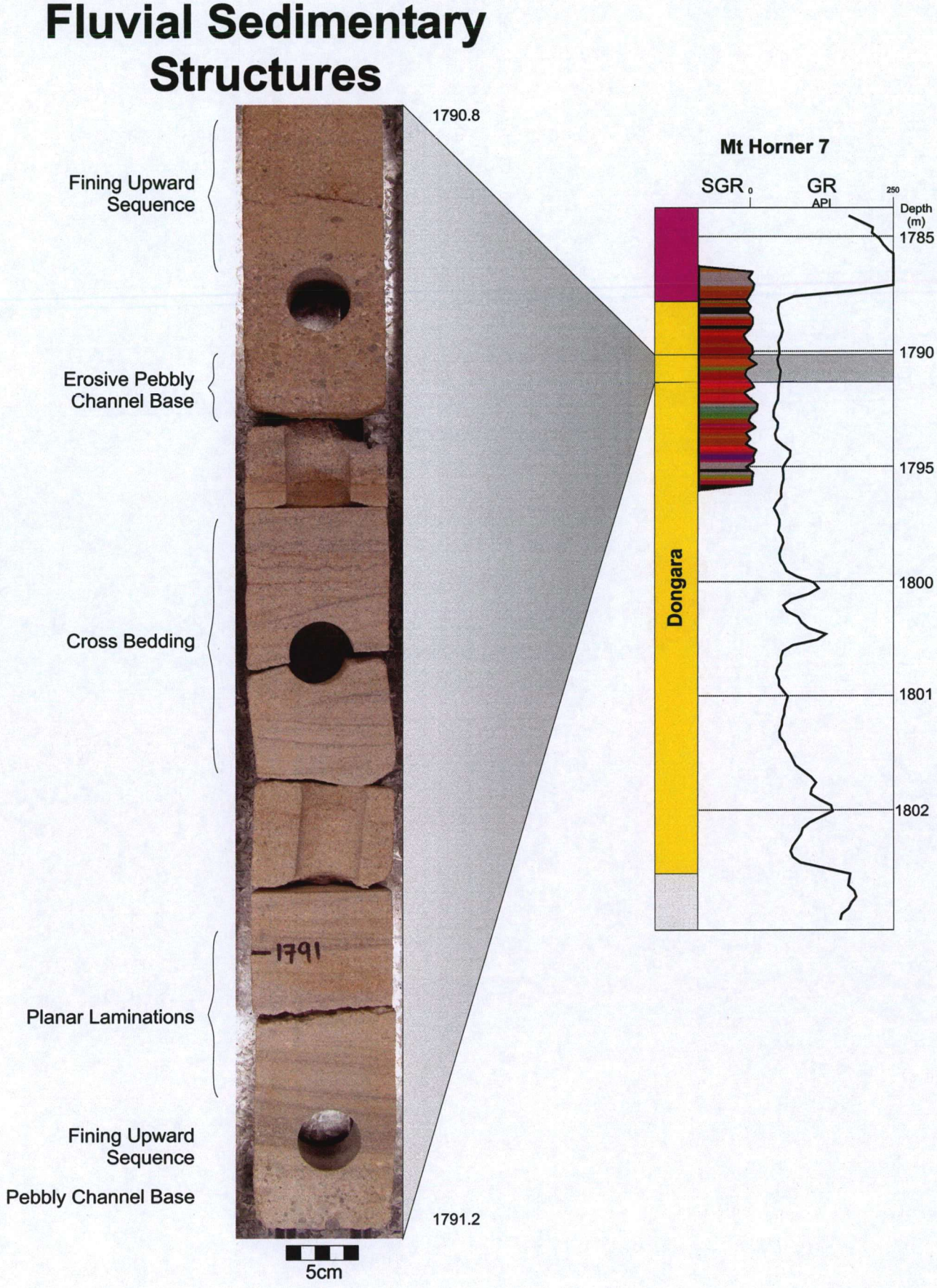

Figure 6.5 Typical fluvial sedimentary structures, as demonstrated in core from Mt Horner 7.

6.1.3 *D. parvithola* Sediment Package

D. parvithola is the uppermost sediment package, however, its beach facies is still yet to be constrained. The proposed beach environment associated with this sediment package is thought to lie in an area north of the Dongara Terrace, but unfortunately no wells have intersected it. The *D. parvithola* palynozone is latest Permian in age (Fig. 2.1). Sediments of this age may represent the final stages of sea level rise before the more pronounced Earliest Triassic marine transgression. In such an environment, only a thin beach section may have been preserved, or conversely, no beach sediments may have been preserved at all. Cores from Jingemia 4 display a thick, quartz-rich interval with nearshore marine sedimentary structures. These are interpreted as transgressive sands that possibly constitute the *D. parvithola* sediment package. With no palynology data in the late Permian sediments of the Jingemia wells, this interpretation is still considered uncertain. The palaeogeography for this time interval is highly speculative, because the beach zone has not been defined by well intersection. Due to this uncertainty, no palaeogeography maps of this sediment package were constructed.

6.2 Palaeogeographic Evolution

Figure 6.3 displays a cross-section of the available SGR and wireline total GR data. Annotated on this cross section is the interpretation of the two *D. ericanus* beaches and the associated fluvial and shoreface sediments surrounding them (Fig. 6.3). A schematic representation of the palaeogeographic evolution can be viewed in Figure 6.6.

From the lateral distribution of these facies, the beach depositional environment is seen to back-step towards the north during the late Permian (Fig. 6.6). The distribution of these beaches throughout the late Permian is interpreted to result from a marine transgression. As the sea level progressively rose, the *D. ericanus* 1 sediment package was drowned, and was overlain by *D. ericanus* 2 sediments. A further rise in sea level again drowned the palaeo-shoreline, and the *D. Parvithola* sediments were in turn deposited. This latest rise in sea level is thought to be the last eustatic

fluctuation before major rapid marine transgression in the early Triassic. The proposed accommodation vs. time curve of this sequence of events is displayed in the inset of Figure 6.6.

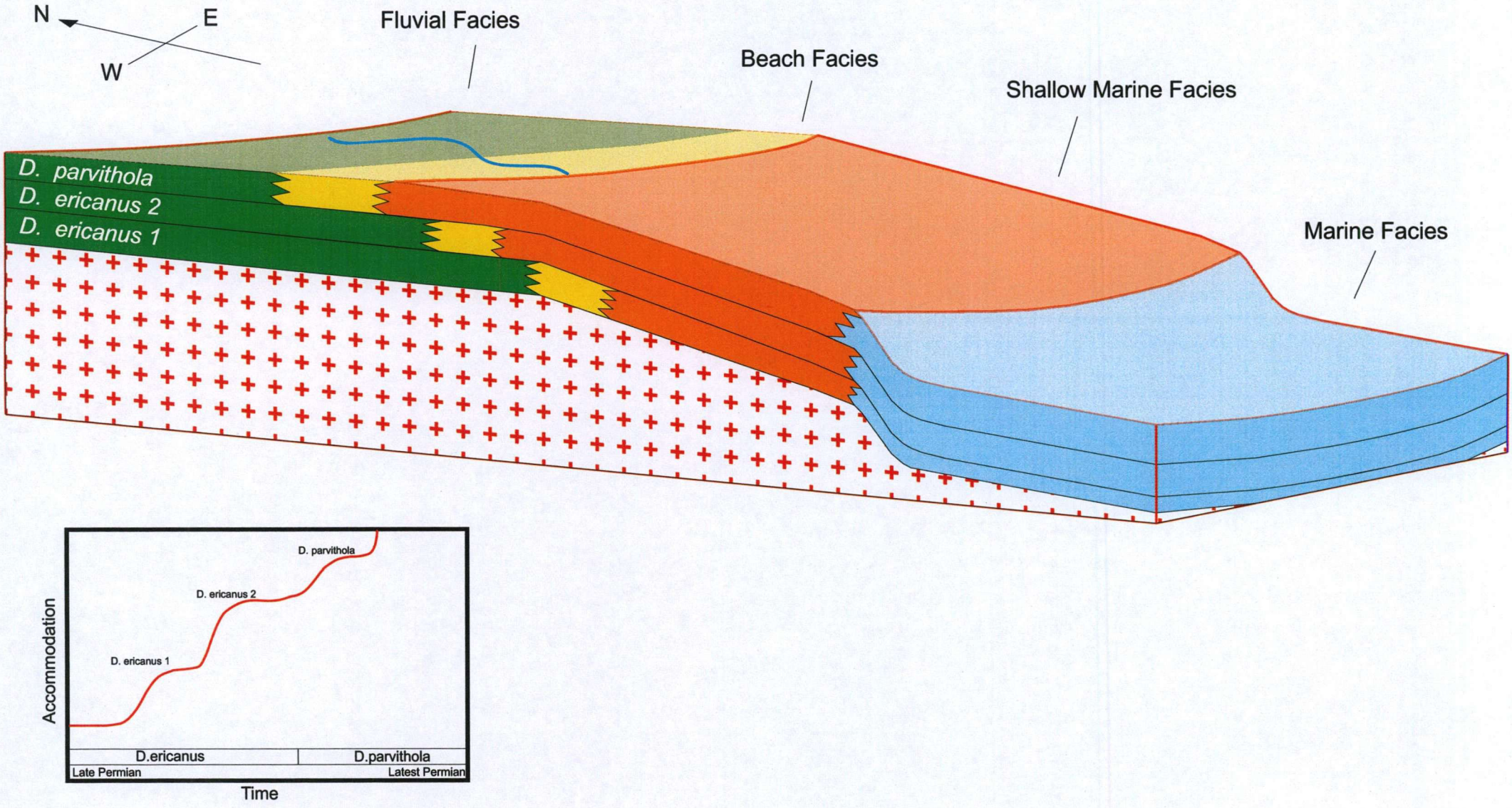

Figure 6.6 A schematic representation of the palaeogeographic evolution through the late Permian. Note the back-stepping shoreline throughout the late Permian. The sediment accommodation vs. time curve of this evolution is inset

7 CONCLUSIONS AND RECOMMENDATIONS

7.1 Conclusions

Core SGR data (when acquired in accordance with the methodology outlined in this study) is adequately precise and is comparable in resolution with wireline SGR data. In instances where wells are lacking wireline SGR data, core SGR data provides an effective substitute and can be confidently used in its place.

The repeatability study demonstrated the inherent errors within the core SGR data that at first appeared substantial. Due to the small number of repeated samples, these errors are regarded as unconstrained. Core SGR data has proven itself as sufficiently precise by the fact that it could be confidently tied in with wireline SGR data from adjacent wells of the same field.

Spectral gamma ray data analysis is an efficient and effective tool in high-resolution correlation within the Permian Dongara Sandstone, and is particularly useful for facies correlations of thorium-rich beach deposits. The distributions of such beaches can be mapped using this technique, and these beaches provide a positive facies anchor when generating palaeofacies maps. These palaeofacies maps are best constrained when integrated with characteristic sedimentary structures observed in core. The orientation of these beaches can define the palaeogeography, and the study of how the palaeogeography changes with time can be applied in the construction of a sequence stratigraphic framework for the Dongara Sandstone.

From analysis of SGR data and core descriptions, the Dongara Sandstone is thought to be a back-stepping shoreface sandstone, deposited during a transgressive systems tract. Marine transgression occurring in the late Permian, just prior to the rapid early Triassic marine transgression, is thought to be the driving force behind such a depositional history.

The techniques applied in this study need not be specific to the Perth Basin. In situations where the reservoir has hot sand intervals, SGR analysis can be applied to further refine intra-formational characterisation and correlation. Again, this level of correlation detail is something that cannot be achieved using total GR logs.

7.2 Recommendations for Future Research

Wireline SGR logs are strongly recommended to be run in all upcoming wells in the northern Perth Basin. With additional SGR data, the spatial distributions of facies can be further constrained and greater confidence can be assigned to correlations. With greater confidence in interpreted facies distributions, a detailed sequence stratigraphic framework for the Dongara Sandstone can be constructed.

Sidewall cores are more commonly taken throughout the whole reservoir interval, however, because of the small sample size, the usefulness of SGR analysis of these appears limited. One possible method for obtaining SGR data from sidewall cores is to analyse the sample for a very long counting time, in isolation from external contamination. This process has the potential to harness the SGR signature of small samples of rock, however, to the best of the author's knowledge, this idea has not been previously tested.

Further radioelement analysis could be conducted on sidewall cores using inductively coupled plasma (ICP) techniques, since this technique uses only small volumes of rock sample. Svendsen and Hartley (2001) regard data from this technique as being comparable with SGR data. With a greater coverage of sidewall cores than full-hole cores, a more extensive radioelement database from the whole reservoir interval would result.

Existing palynological data formed the basis of the interpretations made, however, these data are sporadic. Techniques that can further constrain chronostratigraphy would be a welcome addition to the interpretations made in this study.

Bioturbation was commonly identified in cores, however, this was not extensively studied. Detailed ichnological studies of cores from the Perth Basin may shed further light on any other palaeoenvironmental factors such as water depth, climate and sedimentation rates at time of deposition; information which may further validate regional palaeogeography maps.

Further advances in palaeogeographic mapping can better constrain the depositional environment of the Dongara Sandstone, and therefore predictions on sand distribution and reservoir quality can be made with greater confidence. The SGR technique can be used as a valuable tool in reducing the vast uncertainties encountered when drilling exploration wells, not just within the Perth Basin, but throughout the world.

8 REFERENCES

Adams, J.A.S., and Weaver, C.E., 1958. Thorium-to-uranium ratios as indicators of sedimentary processes: example of concept and geochemical facies: Bulletin of American Association Petroleum Geologists, v. 42, pp. 387-430.

Aigner, T., Schauer, M., Junghans, W.-D., and Reinhardt, L., 1995. Outcrop gamma-ray logging and its applications: examples from the German Triassic. Sedimentary Geology., v. 100, pp. 47-61.

Baker Atlas. 1992. Introduction to Wireline Log Analysis. Western Atlas International, Inc., Houston, Texas. pp. 217-221.

Buswell, A.J., Powell, W.D., and Sholefield, T., 2004. The northern Perth Basin – From marginally prospective for gas to highly prospective for both oil and gas: APPEA Journal, v. 44, pp. 181-200.

Cawood, P.A., and Nemchin, A.A., 2000. Provenance record of a rift basin: U/Pb ages of detrital zircons from the Perth Basin, Western Australia: Sedimentary Geology, v. 134, pp. 209-234.

Clare, A.P., and Crowley, A.J., 2001. Qualitative analysis of spectral gamma ray data as a tool for fieldwide and regional stratigraphic correlation, Enderby Terrace, Carnarvon Basin, Western Australia: APPEA Journal, v. 41, pp. 449-462.

Crostella, A., 1995. An evaluation of the hydrocarbon potential of the onshore northern Perth Basin: Western Australia Geological Survey, Report 43, 67p.

Davies, S.J., and Elliott, T., 1995. Spectral gamma ray characterization of high resolution sequence stratigraphy: examples from Upper Carboniferous

fluvio-deltaic systems, County Clare, Ireland. In: High resolution sequence stratigraphy: Innovations and applications (Ed. By J.A. Howell and J.F. Aitken) pp. 25-35. Spec. Publ. Geol. Soc. London. 104.

De Broekert, P.P., Wilde, S.A., and Kennedy, A.K., 2004. Variety, age and origin of zircons in the mid-Cenozoic Westonia Formation, southwest Yilgarn Craton, Western Australia: Australian Journal of Earth Sciences, v. 51, pp. 157-171.

Exploranium. User manual for the GR-256 portable gamma ray spectrometer. (Unpublished text).

Geoscience Australia, 2004. Location map of the Perth Basin. http://www.ga.gov.au/image_cache/GA1559.pdf.

Petrie, E. and others, Geoscience Australia (2003) Oil and Gas Resources of Australia 2002. Geoscience Australia, Canberra.

Harris, L.B., Higgins, R.I., Dentith, M.C., and Middleton, M.F., 1994. transtentional analogue modelling applied to the Perth Basin, Western Australia. In: Purcell, P.G. and R.R (Eds.) The sedimentary basins of Western Australia, 1994 edition.

Hurst, A., and Milodowski, A., 1996. Thorium distribution in some North Sea sandstones: implications for petrophysical evaluation: Petroleum Geoscience, v. 2, pp. 59-68.

Just, J., 2002. Depositional and diagenetic history of the upper Permian Beekeeper
Formation, Woodada gas field, onshore northern Perth Basin, Western Australia: Honours thesis, University of Western Australia, Perth, 95p.

Morton, A.C., and Hallsworth, C.R., 1999. Processes controlling the composition of heavy mineral assemblages in sandstones: Sedimentary Geology, v. 124, pp. 3-29.

Mory, A.J., and Iasky, R.P., 1996. Stratigraphy and structure of the onshore northern Perth Basin: Western Australia Geological Survey, Report 46, 101p.

Owad-Jones, D.L., and Ellis, G.K., 2000. Western Australia atlas of petroleum fields, onshore Perth Basin: Petroleum Division, DMEWA. Vol. 1.

Prinz, M., Harlow, G., and Peters, J., (Eds) 1978. Simon and Schuster's guide to rocks and minerals. Simon and Schuster Inc.

Rasmussen, B., Glover, J.E., and Alexander, R., 1989. Hydrocarbon rims on monazite in Permian-Triassic arenites, northern Perth Basin, Western Australia: Pointers to the former presence of oil: Geology, v. 17, pp. 115-118.

Reid, I., and Frostick, L.E., 1985. Role of settling, entrainment and dispersive equivalence and interstice trapping in placer formation: J. Geol. Soc. London, v. 142, pp. 739-746.

Rider, M.H., 1996. The geological interpretation of well logs. Whittles Publishing pp. 67-91.

Ruffell, A., and Worden, R., 2000. Palaeoclimate analysis using spectral gamma-ray data from the Aptian (Cretaceous) of southern England and southern France: Palaeogeography, Palaeoclimatology, Palaeoecology, v. 155 pp. 265-283.

Saunders, D.F., Burson, K.R., Branch, J.F., and Thompson, K.C., 1993. Relation of thorium-normalised surface and aerial radiometric data to subsurface petroleum accumulations: Geophysics, v. 58, No. 10. pp. 1417-1427.

Song, T., and Cawood, P.A., 2000. Structural styles in the Perth Basin associated with the Mesozoic break-up of Greater India and Australia: Tectonophysics, v. 317 pp. 55-72.

Svendsen, J.B., and Hartley, N.R., 2001. Comparison between outcrop-spectral gamma ray logging and whole rock geochemistry: implications for quantitative reservoir characterisation in continental sequences: Marine and Petroleum Geology, v. 18, pp. 657-670.

Thomas, B.M., and Barber, C.J., 2004. A re-evaluation of the hydrocarbon habitat of the northern Perth Basin: APPEA Journal, v. 44, pp.59-92.

WAPET Exploration Review, 1996. Unpublished text.

Wilford, J.R., Dent, D.L., Dowling, T., and Braaten, R., 2001. Rapid mapping of salt stores using airborne radiometrics and digital elevation models: AGSO Research Newsletter, May edition, pp. 33-40.

9 APPENDIX

(Note. All well SGR data is contained in the contained in digital form on the attached CD)

Histograms of the whole core database

Uranium histogram

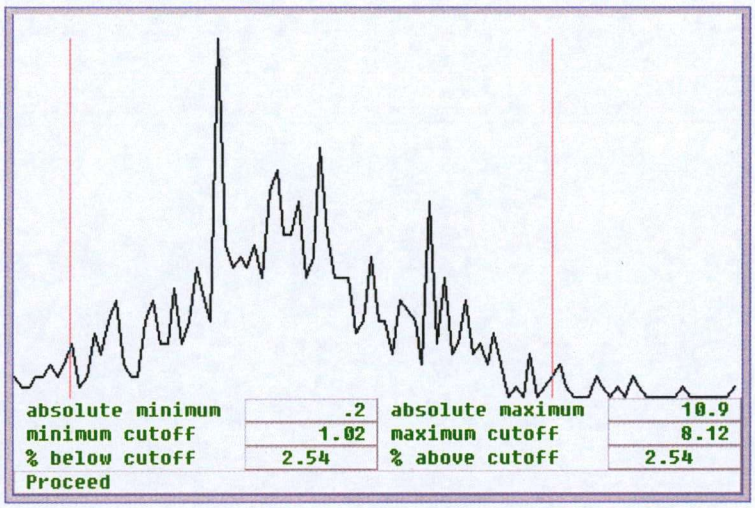

Thorium histogram

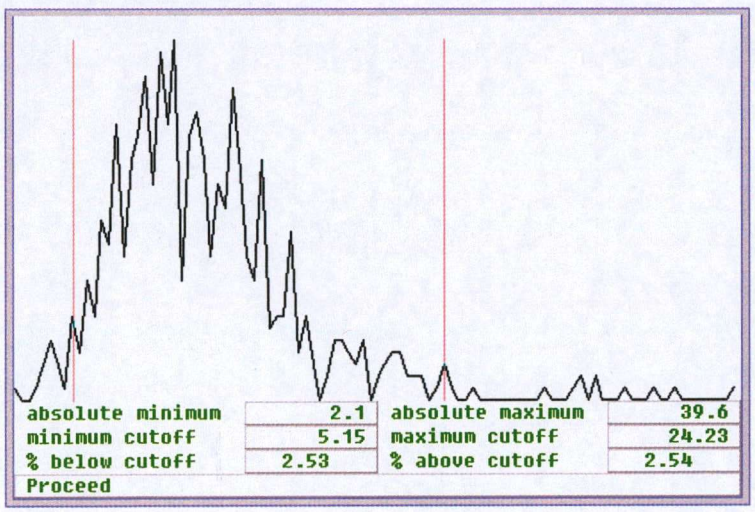

Potassium histogram